Formulation and users' guide for Q-GCM (version 1.0)

A. McC. Hogg, J. R. Blundell, W. K. Dewar and P. D. Killworth

March 25, 2003

Contents

1 Introduction **3**

2 Quasi-Geostrophic equations **3**

3 Mixed layers **7**
3.1 Mixed layer stress 7
3.2 Mixed layer evolution 9

4 Flux between layers **9**
4.1 Incoming solar flux 10
4.2 Radiative fluxes 10
4.3 Sensible and latent heat flux 12
4.4 Entrainment heat flux 12

5 Layer equations **13**
5.1 Ocean layer 1 13
5.2 Ocean layer 2 14
5.3 Ocean mixed layer 14
5.4 Atmosphere layer 1 14
5.5 Atmosphere layer 2 15
5.6 Atmosphere mixed layer 15
5.7 Convection 15

6 Mean state **15**

7 Final equation set **16**

8 Numerical formulation **20**
8.1 Discretisation in space and time 20
8.2 Effect of the Laplacian operator on a Fourier component 21
8.3 Solution of the Helmholtz equation 22
8.4 Integration routines 24
8.5 Diffusive timescales 24

9 Users' guide **25**
9.1 Components of the code 25
9.2 Compiling the code 26
9.3 Structure of the code 26
9.3.1 Input files 27
9.3.2 Program structure 27

9.3.3 Output files . . . 27
9.3.4 Location of variables . . . 29
9.3.5 Diagnostics . . . 29
9.3.6 Default case . . . 29
9.3.7 Possible problems . . . 29
9.3.8 Feedback and future plans . . . 30

A Writing radiation as a perturbation to mean state 31
A.1 Functional form of radiation parameters . . . 31
A.2 Rules for linearising . . . 31
A.3 Calculations . . . 32

B Constraints on mass and momentum 34
B.1 Ocean constraints . . . 34
B.2 Atmospheric momentum constraints . . . 34

C Application of boundary conditions 36

D Starting at radiative equilibrium 37

E Kinetic Energy 38

Abstract

The design and implementation of a mid-latitude coupled climate model is described. The basic model consists of a quasi-geostrophic channel atmosphere coupled to a simple, rectangular quasi-geostrophic ocean. Heat and momentum exchanges between the ocean and the atmosphere are mediated via mixed layer models and the system is driven by latitudinally dependent incident solar radiation.

1 Introduction

In this document we describe the formulation of an intermediate complexity mid-latitude coupled climate model. The model uses quasi-geostrophic (QG) dynamics in both ocean and atmosphere so that the momentum equations can be solved quickly, while non-linear dynamics and high resolution in the ocean can be retained.

Quasi-geostrophy is known to be a robust approximation to ocean and atmosphere mesoscale dynamics, explicitly involves relative vorticity and eddies, and is much more dynamically transparent than the primitive equations. Further, such a model stands on some twenty odd years of experimentation in ocean-only and atmosphere-only settings and thus represents a logical next step in the continued use of quasi-geostrophy for process modelling. However, QG models are not naturally suited to be run in coupled scenarios because of the poor representation of vertical fluxes of heat, and advection of temperature. An exception is ECBilt (Opsteegh et al., 1998), a 3 layer QG atmosphere model which has been coupled to an ocean model; however the evolution of temperature at the ocean-atmosphere boundary and representation of diabatic processes is oversimplified. Kravtsov and Robertson (2002) describe a coupled QG model which includes an oceanic mixed layer to better represent ocean heat transport. We extend this concept by including mixed layers in both ocean and atmosphere components of a layered QG model. The mixed layers allow the communication of stress and the flux of heat between ocean and atmosphere. The coupling of an atmosphere QG model to an ocean QG model then involves the connection of two anti-symmetric models which use the same equations but different governing parameters. In this way we can model a channel atmosphere coupled to a box ocean, and use this model to simulate a mid-latitude climate system driven by latitudinal variations in incoming radiation. A two layer version of the Quasi-Geostrophic Coupled Model (Q-GCM) is shown schematically in figure 1.

2 Quasi-Geostrophic equations

Begin with the equations for conservation of momentum in a rotating fluid,

$$u_t + uu_x + vu_y + wu_z - fv = -p_x + Ku_{xx} + Ku_{yy} + Ku_{zz}, \tag{2.1a}$$

$$v_t + uv_x + vv_y + wv_z + fu = -p_y + Kv_{xx} + Kv_{yy} + Kv_{zz}, \tag{2.1b}$$

$$w_t + uw_x + vw_y + ww_z = -p_z - g + Kw_{xx} + Kw_{yy} + Kw_{zz}, \tag{2.1c}$$

where we have used $\mathbf{u} = (u, v, w)$ for velocity, and subscripts to represent partial derivatives. The pressure p has been rescaled by mean density $\overline{\rho}$ and we represent viscosity using a constant diffusion coefficient K. The Coriolis parameter has been represented by f and gravitational acceleration by g. The other equations required here are the continuity equation

$$u_x + v_y + w_z = 0, \tag{2.2}$$

and the mass conservation equation which we write as

$$\rho_t + u\rho_x + v\rho_y + w\rho_z = K_H\rho_{xx} + K_H\rho_{yy} + K_V\rho_{zz}. \tag{2.3}$$

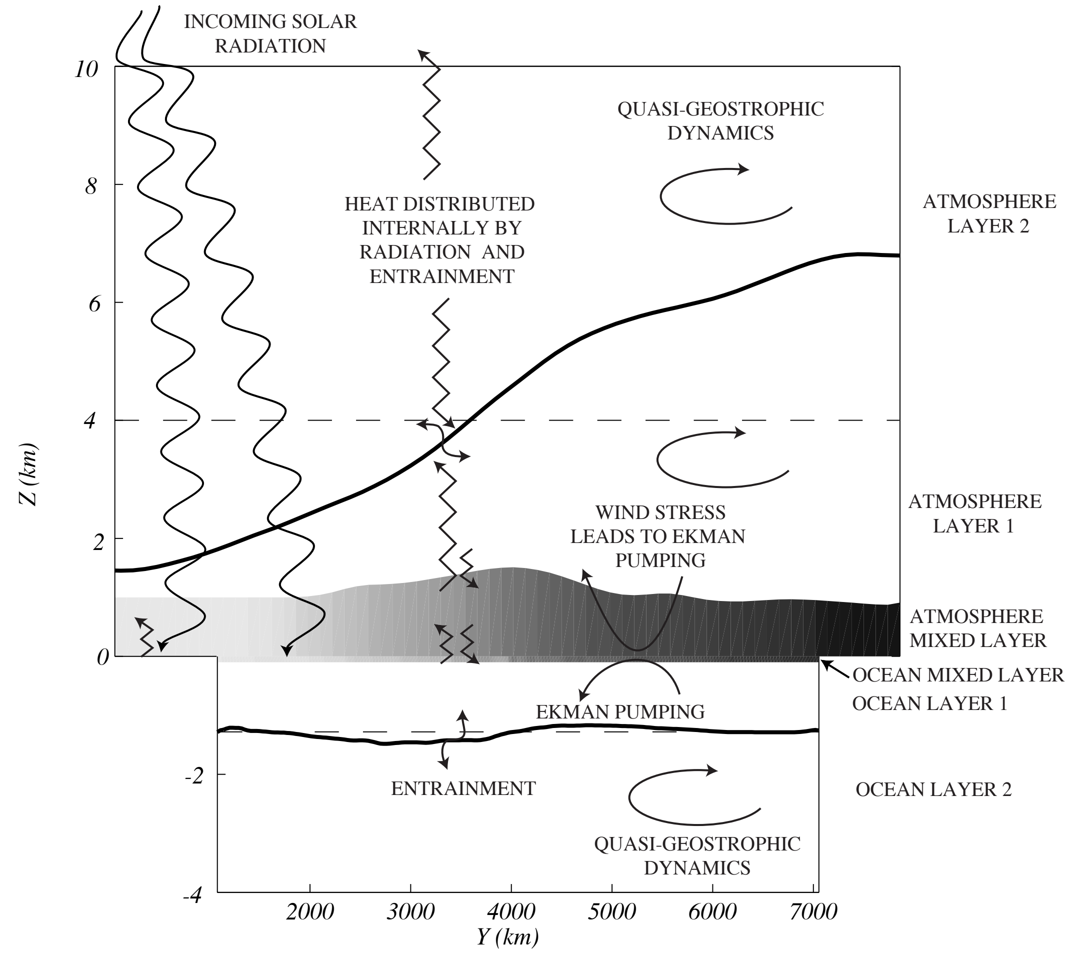

Figure 1: Schematic of the Quasi-Geostrophic Coupled Model. This meridional slice through the model shows the interface dividing the two QG dynamical layers in both the ocean and the atmosphere. The mixed layers, shown by the shading which respresents temperature, act to distribute heat and momentum between the two domains. The model is driven by latitudinally varying solar forcing, and by redistribution of heat by longwave radiation in the atmosphere.

To derive the quasi-geostrophic equations which govern the model dynamics, we simplify (2.1)–(2.3). This could be done rigorously by first non-dimensionalising, and then by scaling away less important terms, but it will suffice for now to do this informally. We begin by assuming, for the purposes of finding the zeroth order equations, that

1. Vertical velocity is small compared with horizontal velocities;
2. The Coriolis parameter is represented by the frozen β-plane approximation $f(y) = f_0 + \beta y$ where f_0 represents the zeroth order effect of rotation;
3. Diffusion of momentum is dominated by pressure gradients.

The zeroth order equations in which pressure balances rotation are then

$$f_0 {}^a v_1 = {}^a p_{1x}, \tag{2.4a}$$

$$f_0 {}^a u_1 = -{}^a p_{1y}, \tag{2.4b}$$

$${}^a p_{1z} = -g, \tag{2.4c}$$

and the continuity equation is

$${}^a u_{1x} + {}^a v_{1y} = 0 \tag{2.5}$$

which is automatically satsfied by (2.4a) and (2.4b). Vorticity is given by

$$ {}^a v_{1x} - {}^a u_{1y} = \frac{\nabla_H^2 {}^a p_1}{f_0}. \tag{2.6} $$

The notation used here indicates that we are referring to layer 1 (subscript 1) in the atmosphere (superscript a). Subscript m is used to represent the mixed layer. The same notation is used for quantities which refer to interface properties, with the ocean-atmosphere boundary defined as interface 0. In the atmosphere (ocean), interface 1 is defined to be on the upper (lower) boundary of layer 1.

We can now compute the first order quantities (signified by * in the equations below) for the horizontal momentum and continuity equations which include zeroth order horizontal velocity terms and first order pressure and rotation terms,

$$ {}^a u_{1t} + {}^a u_1 {}^a u_{1x} + {}^a v_1 {}^a u_{1y} - f_0 {}^a v_1{}^* - \beta y {}^a v_1 = -{}^a p_{1x}^* - {}^a A_H \nabla_H^4 {}^a u_1, \tag{2.7a} $$

$$ {}^a v_{1t} + {}^a u_1 {}^a v_{1x} + {}^a v_1 {}^a v_{1y} + f_0 {}^a u_1{}^* + \beta y {}^a u_1 = -{}^a p_{1y}^* - {}^a A_H \nabla_H^4 {}^a v_1, \tag{2.7b} $$

$$ {}^a u_{1x}^* + {}^a v_{1y}^* + {}^a w_{1z}^* = 0, \tag{2.8} $$

where we have introduced a fourth-order horizontal viscosity scheme (the coefficient ${}^a A_H$ is positive for energy dissipation). First order pressure terms can be eliminated by cross-differentiating (2.7a) and (2.7b), giving

$$ \begin{aligned} &{}^a u_{1ty} + ({}^a u_1 {}^a u_{1x})_y + ({}^a v_1 {}^a u_{1y})_y - f_0 {}^a v_{1y}^* - (\beta y {}^a v_1)_y + {}^a A_H \nabla_H^4 {}^a u_{1y} \\ &\quad = {}^a v_{1tx} + ({}^a u_1 {}^a v_{1x})_x + ({}^a v_1 {}^a v_{1y})_x + f_0 {}^a u_{1x}^* + (\beta y {}^a u_1)_x + {}^a A_H \nabla_H^4 {}^a v_{1x}, \end{aligned} \tag{2.9} $$

and rearranging:

$$ \begin{aligned} &\left(\frac{\nabla_H^2 {}^a p_1}{f_0} + \beta y\right)_t + \left({}^a u_1 \left[\frac{\nabla_H^2 {}^a p_1}{f_0} + \beta y\right]\right)_x + \left({}^a v_1 \left[\frac{\nabla_H^2 {}^a p_1}{f_0} + \beta y\right]\right)_y + \\ &\quad ({}^a u_{1x} + {}^a v_{1y}) \left(\frac{\nabla_H^2 {}^a p_1}{f_0} + \beta y\right) + f_0({}^a u_{1x}^* + {}^a v_{1y}^*) = -{}^a A_H \nabla_H^4 \left(\frac{\nabla_H^2 {}^a p_1}{f_0}\right) \end{aligned} \tag{2.10} $$

Insert (2.5) and (2.8) to eliminate zeroth order divergence terms and first order velocities, leaving an equation which depends only upon zeroth order terms

$$ \left(\frac{\nabla_H^2 {}^a p_1}{f_0} + \beta y\right)_t + \left({}^a u_1 \left[\frac{\nabla_H^2 {}^a p_1}{f_0} + \beta y\right]\right)_x + \left({}^a v_1 \left[\frac{\nabla_H^2 {}^a p_1}{f_0} + \beta y\right]\right)_y = f_0 {}^a w_{1z}^* - \frac{{}^a A_H}{f_0} \nabla_H^6 {}^a p_1. \tag{2.11} $$

We now integrate (2.11) over the layer depth. Note that it is assumed that ${}^a p_1$, ${}^a u_1$ and ${}^a v_1$ are effectively layer-averaged quantities, so that integration between zero and ${}^a H_1$ simply gives

$$ \left(\frac{\nabla_H^2 {}^a p_1}{f_0}\right)_t + \left({}^a u_1 \frac{\nabla_H^2 {}^a p_1}{f_0}\right)_x + \left({}^a v_1 \left(\frac{\nabla_H^2 {}^a p_1}{f_0} + \beta y\right)\right)_y = \frac{f_0({}^a w_1{}^* - {}^a w_m{}^*)}{{}^a H_1} - \frac{{}^a A_H}{f_0} \nabla_H^6 {}^a p_1, \tag{2.12} $$

which is an equation for the evolution of potential vorticity in the layer. Evaluation of vertical velocity at the layer boundaries (${}^a w_1{}^*$ and ${}^a w_m{}^*$) requires knowledge of the flux between layers (which we call e for net entrainment velocity through the boundary of the layer). Vertical velocity is a first order quantity and thus incorporates variable layer thickness ${}^a h_1$, giving

$$ {}^a w_1{}^* = {}^a h_{1t} + ({}^a u_1 {}^a h_1)_x + ({}^a v_1 {}^a h_1)_y + {}^a e_1. \tag{2.13} $$

The lower boundary of the atmosphere is solid; however vertical velocity due to Ekman pumping (derived below) makes a contribution; ${}^a w_m{}^* = {}^a w_{ek}$. We can now write an equation for the lower atmospheric layer dynamics,

$$ {}^a q_{1t} + ({}^a u_1 {}^a q_1)_x + ({}^a v_1 {}^a q_1)_y = \frac{f_0({}^a e_1 - {}^a w_{ek})}{{}^a H_1} - \frac{{}^a A_H}{f_0} \nabla_H^6 {}^a p_1, \tag{2.14} $$

where layer potential vorticity is defined as

$$ {}^a q_1 \equiv \frac{\nabla_H^2 {}^a p_1}{f_0} + \beta y - \frac{f_0 {}^a \eta_1}{{}^a H_1}, \tag{2.15} $$

and the perturbation interface height, ${}^a \eta_1 \equiv {}^a h_1 - {}^a H_1 = \frac{{}^a p_1 - {}^a p_2}{{}^a g'}$. Equivalent equations can be derived for each layer in the model. For a two layer model these are:

$$ {}^a q_{2t} + ({}^a u_2 {}^a q_2)_x + ({}^a v_2 {}^a q_2)_y = -\frac{f_0}{{}^a H_2} {}^a e_1 - \frac{{}^a A_H}{f_0} \nabla_H^6 {}^a p_2, \tag{2.16} $$

where

$$ {}^a q_2 \equiv \frac{\nabla_H^2 {}^a p_2}{f_0} + \beta y + \frac{f_0 {}^a \eta_1}{{}^a H_2}, \tag{2.17} $$

and for the ocean,

$$ {}^o q_{1t} + ({}^o u_1 {}^o q_1)_x + ({}^o v_1 {}^o q_1)_y = \frac{f_0}{{}^o H_1}({}^o w_{ek} - {}^o e_1) - \frac{{}^o A_H}{f_0} \nabla_H^6 {}^o p_1, \tag{2.18} $$

$$ {}^o q_{2t} + ({}^o u_2 {}^o q_2)_x + ({}^o v_2 {}^o q_2)_y = \frac{f_0}{{}^o H_2} \left({}^o e_1 - \frac{\delta_e}{2 f_0} \nabla_H^2 {}^o p_2 \right) - \frac{{}^o A_H}{f_0} \nabla_H^6 {}^o p_2, \tag{2.19} $$

where

$$ {}^o q_1 \equiv \frac{\nabla_H^2 {}^o p_1}{f_0} + \beta y + \frac{f_0 {}^o \eta_1}{{}^o H_1}, \tag{2.20} $$

$$ {}^o q_2 \equiv \frac{\nabla_H^2 {}^o p_2}{f_0} + \beta y - \frac{f_0 {}^o \eta_1}{{}^o H_2}, \tag{2.21} $$

$$ {}^o \eta_1 = -\frac{{}^o p_1 - {}^o p_2}{{}^o g'}. \tag{2.22} $$

The boundary conditions in the model are mixed conditions following Haidvogel et al. (1992). The conditions are applied to the pressure field, and are written for the example of the north and south boundaries of the lower atmosphere to be

$$ {}^a p_1 = {}^a f_1(t), \tag{2.23} $$

$$ {}^a p_{1nn} = -{}^a \alpha {}^a p_{1n}, \tag{2.24} $$

$$ {}^a p_{14n} = -{}^a \alpha {}^a p_{13n}, \tag{2.25} $$

where the coefficient ${}^a \alpha$ is zero for free slip and large for no-slip boundary conditions and subscript n represents the outward normal derivative. The function ${}^a f_1(t)$ is determined using constraints on mass and momentum, after McWilliams (1977), and will be different on the northern and southern boundaries in the atmosphere depending upon the net flow in the layer. These conditions are derived in appendix B.2. The east and west boundaries are periodic. The ocean boundaries are treated using the same mixed boundary conditions described by (2.23)–(2.25), with the x-derivative of pressure used on the east and west boundaries. The value of ${}^o f_1(t)$ is constrained by mass conservation and is the same for all boundaries.

3 Mixed layers

Quasi-geostrophy describes, to first order, the dynamics of both ocean and atmosphere, but cannot handle the fluxes of heat and momentum between these two domains which are required for a coupled model. Q-GCM avoids this difficulty by embedding mixed layers within layer 1 of both ocean and atmosphere. In its current form the mixed layers do not include parametrisation of humidity in the atmosphere or salinity in the ocean, and therefore exchanges of these quantities are not modelled. Nonetheless, the most fundamental processes – transfer of momentum from atmosphere to ocean, and flux of heat in both directions – are included.

3.1 Mixed layer stress

We first derive the stress at the ocean-atmosphere interface by finding the atmospheric mixed layer velocities. The distinction between mixed layer and layer 1 velocities is that the mixed layer is thin enough that the vertical flux of horizontal momentum is significant. The zeroth order momentum equations can be found by including the vertical flux of momentum by a dynamic stress (rescaled by mean density ${}^a\rho$)

$$-f_0{}^a v_m = -{}^a p_{1x} + {}^a\tau_z^x, \tag{3.1a}$$

$$f_0{}^a u_m = -{}^a p_{1y} + {}^a\tau_z^y. \tag{3.1b}$$

Assuming a fixed atmospheric mixed layer thickness and zero stress at the upper boundary of the mixed layer, we substitute (2.4a,b) and integrate over mixed layer depth ${}^aH_m$ to give

$${}^a v_m = {}^a v_1 + \frac{{}^a\tau^x}{{}^aH_m f_0}, \tag{3.2a}$$

$${}^a u_m = {}^a u_1 - \frac{{}^a\tau^y}{{}^aH_m f_0}, \tag{3.2b}$$

where it is implied that stress is a layer-averaged quantity. We assume stress is a quadratic function of the ageostrophic mixed layer velocity (Pedlosky, 1987),

$$({}^a\tau^x, {}^a\tau^y) = C_D|\mathbf{{}^au_m}|({}^a u_m, {}^a v_m), \tag{3.3}$$

C_D being a dimensionless drag coefficient. Substituting (3.3) into (3.2a,b) gives

$${}^a v_m = {}^a v_1 + \frac{C_D|\mathbf{{}^au_m}|{}^a u_m}{{}^aH_m f_0}, \tag{3.4a}$$

$${}^a u_m = {}^a u_1 - \frac{C_D|\mathbf{{}^au_m}|{}^a v_m}{{}^aH_m f_0}. \tag{3.4b}$$

which allows us to write, with some algebraic manipulation,

$${}^a v_m = \left[{}^a v_1 + \frac{C_D|\mathbf{{}^au_m}|{}^a u_1}{{}^aH_m f_0}\right]\left[1 + \left(\frac{C_D|\mathbf{{}^au_m}|}{{}^aH_m f_0}\right)^2\right]^{-1}, \tag{3.5a}$$

$${}^a u_m = \left[{}^a u_1 - \frac{C_D|\mathbf{{}^au_m}|{}^a v_1}{{}^aH_m f_0}\right]\left[1 + \left(\frac{C_D|\mathbf{{}^au_m}|}{{}^aH_m f_0}\right)^2\right]^{-1}, \tag{3.5b}$$

allowing direct calculation of stress provided one has calculated

$$|\mathbf{{}^au_m}| \equiv \sqrt{{}^a u_m{}^2 + {}^a v_m{}^2} = \left(\frac{\sqrt{2}\,C_D}{{}^aH_m f_0}\right)^{-1}\sqrt{-1 + \sqrt{1 + 4\left(\frac{C_D|\mathbf{{}^au_1}|}{{}^aH_m f_0}\right)^2}}. \tag{3.6}$$

A second distinction between mixed layer and layer 1 velocities exists because the ageostrophic mixed layer velocities have a divergent component which produces vertical Ekman velocities. Ekman pumping is calculated using the continuity equation (2.2) integrated from 0 to ${}^aH_m$,

$$ {}^aw_{ek} = -{}^aH_m{}^au_{mx} - {}^aH_m{}^av_{my}, \tag{3.7} $$

where we use ${}^aw_m(0) = 0$ and ${}^aw_m({}^aH_m) = {}^aw_{ek}$. Substitute velocity from (3.2a,b),

$$ {}^aw_{ek} = \frac{{}^a\tau^y_x - {}^a\tau^x_y}{f_0}, \tag{3.8} $$

the familiar expression for Ekman velocity as a function of stress.

The ocean mixed layer is essentially an inversion of the atmospheric mixed layer. The difference here is that stress in the oceanic mixed layer is passive, depending entirely on wind stress and the atmosphere to ocean density ratio,

$$ {}^o\tau = \xi\frac{{}^a\rho}{{}^o\rho}{}^a\tau, \tag{3.9} $$

where ξ is an order 1 stress multiplier and is designed to take into account the poor vertical resolution of the atmosphere into account. Ekman pumping in the ocean surface layer can be calculated from stress in the same way as (3.8) to give

$$ {}^ow_{ek} = \frac{{}^o\tau^y_x - {}^o\tau^x_y}{f_0}. \tag{3.10} $$

It is relevant at this stage to note that momentum must also be lost from the ocean, and that this occurs via drag due to a no-slip condition at the ocean floor. We calculate this by assuming an Ekman layer of prescribed thickness $\delta_e = \sqrt{K/f_0}$ and proceed as above. On this occasion there is no need to calculate stress explicitly, and so we determine the Ekman pumping directly from pressure. Velocity in the Ekman layer will be given by

$$ {}^ov_2 = \frac{{}^op_{2x}}{f_0} + \frac{\tau^x}{\delta_e f_0}, \tag{3.11a} $$

$$ {}^ou_2 = -\frac{{}^op_{2y}}{f_0} - \frac{\tau^y}{\delta_e f_0}. \tag{3.11b} $$

We use linear stress,

$$ (\tau^x, \tau^y) = \frac{K}{\delta_e}({}^ou_2, {}^ov_2), \tag{3.12} $$

so that

$$ {}^ov_2 = \frac{{}^op_{2x}}{f_0} + {}^ou_2, \tag{3.13a} $$

$$ {}^ou_2 = -\frac{{}^op_{2y}}{f_0} - {}^ov_2. \tag{3.13b} $$

Combining these two we can write separate equations for each component of velocity,

$$ {}^ov_2 = \frac{{}^op_{2x}}{2f_0} - \frac{{}^op_{2y}}{2f_0}, \tag{3.14a} $$

$$ {}^ou_2 = -\frac{{}^op_{2y}}{2f_0} - \frac{{}^op_{2x}}{2f_0}. \tag{3.14b} $$

This can be substituted into (2.2) and integrated across the Ekman layer:

$$ {}^ow_2 = \frac{\delta_e}{2f_0}\nabla^2_H{}^op_2. \tag{3.15} $$

This vertical velocity on the lower boundary of the ocean alters the vertical velocity in ocean layer 2 but has no impact on the heat flux (as there is no temperature gradient).

3.2 Mixed layer evolution

The mixed layers also act to transfer heat between atmosphere and ocean. To allow this, we need to explicitly calculate the evolution of temperature in the mixed layer. As before we integrate over the mixed layer thickness, but for the purposes of temperature evolution we allow perturbations ${}^a\eta_m = {}^ah_m - {}^aH_m$ to mixed layer height in the atmosphere only. The variable mixed layer height is needed in the atmosphere because of an observed instability which occurs due to large vertical heat transports in regions where there is a coherent pattern of upwelling and cold mixed layer temperatures.

To find the evolution of mixed layer height, we again integrate the continuity equation, this time from 0 to ${}^ah_m$,

$$ {}^aw_m({}^ah_m) = -{}^ah_m{}^au_{mx} - {}^ah_m{}^av_{my}. \tag{3.16} $$

Now we write an equation for the mixed layer height, analogous to (2.13),

$$ {}^aw_m({}^ah_m) = {}^ah_{mt} + {}^au_m{}^ah_{mx} + {}^av_m{}^ah_{my} + {}^ae_m. \tag{3.17} $$

Combining these gives the evolution equation for mixed layer height, which implicitly includes the Ekman divergence terms,

$$ {}^ah_{mt} + ({}^au_m{}^ah_m)_x + ({}^av_m{}^ah_m)_y = -{}^ae_m. \tag{3.18} $$

This equation is solved with ${}^ah_m = {}^aH_m$ on the north and south boundaries.

The evolution of mixed layer temperature comes from a heat equation,

$$ {}^aT_{mt} + {}^au_m{}^aT_{mx} + {}^av_m{}^aT_{my} + {}^aw_m{}^aT_{mz} = {}^aK_H\nabla_H^2{}^aT_m - {}^aK_4\nabla_H^4{}^aT_m - \frac{{}^aF_z}{{}^a\rho{}^aC_p}, \tag{3.19} $$

where ${}^aC_p$ is the specific heat capacity and ${}^aK_H$ a diffusion coefficient. This equation includes a fourth-order diffusion term with coefficient ${}^aK_4$ for numerical stability. We have chosen to retain the horizontal diffusion terms, while writing the vertical diffusion as the vertical gradient of a flux ${}^aF$ of heat energy. Note that flux is defined so that a positive vertical velocity will act to cool the layer in a stably stratified fluid. Integrate (3.19) between 0 and ${}^ah_m$,

$$ {}^aT_{mt} + ({}^au_m{}^aT_m)_x + ({}^av_m{}^aT_m)_y + \frac{{}^aw_{ek}{}^aT_m}{{}^aH_m} = {}^aK_H\nabla_H^2{}^aT_m - {}^aK_4\nabla_H^4{}^aT_m + \frac{-{}^aF_m + {}^aF_0}{{}^a\rho{}^aC_p{}^ah_m}. \tag{3.20} $$

The fluxes at the top of the mixed layer (${}^aF_m$) and at the surface (${}^aF_0$) are derived in §4 below. There is no heat flux on the north and south boundaries.

In the ocean, we use a constant thickness mixed layer, and the equivalent equation to (3.20) is

$$ {}^oT_{mt} + ({}^ou_m{}^oT_m)_x + ({}^ov_m{}^oT_m)_y - \frac{{}^ow_{ek}{}^oT_m}{{}^oH_m} = {}^oK_H\nabla_H^2{}^oT_m + \frac{-{}^oF_0 + {}^oF_m}{{}^o\rho{}^oC_p{}^oH_m}. \tag{3.21} $$

This is solved with zero heat flux on east, west and north boundaries. The southern boundary condition uses ${}^oT_m = {}^oT_S$, a specified constant. This condition is necessary because advection and diffusion of warm tropical water from the south are not explicitly included in the model. A similar boundary condition is not required in the north because convection is active there.

4 Flux between layers

Q-GCM includes flux of heat between each layer due to a number of different processes. We derive each case below, and write heat flux as the superposition of a mean and a first order perturbation quantity, so that fluxes are linearised about a mean state in which the model is in radiative balance.

4.1 Incoming solar flux

The incoming solar radiation is written as a heat flux $F_S = \overline{F_s} + F_s'(y)$. The atmosphere is transparent to incoming shortwave radiation which is deposited directly in the oceanic mixed layer. Over land, incoming shortwave is absorbed by the land and immediately re-emitted as longwave radiation into the atmospheric mixed layer. Heat flux is defined so that positive fluxes denote an upwards movement of heat energy, so that $\overline{F_s}$ is defined negative. We choose the perturbation to radiation so that it integrates to zero over the domain,

$$F_s'(y) = -\left|F_s'\right| \cos\left(\frac{\pi y}{{}^aY}\right), \tag{4.1}$$

where ${}^aY$ is the latitudinal atmospheric domain size.

4.2 Radiative fluxes

Each atmospheric layer, and the oceanic mixed layer, radiates and absorbs heat depending upon its temperature and optical depth. We use the general radiation function

$$B_i(z) = \frac{\sigma}{2}(\overline{T_i} + T_i{}' - \gamma z)^4 \tag{4.2}$$

where γ is the adiabatic lapse rate and $\overline{T_i}$, $T_i{}'$are the mean and perturbation potential temperatures of a layer. The emitted longwave radiation is either absorbed, transmitted or partially transmitted by neighbouring layers. The absorption and emission of each layer is given as below, and details of how these values are derived can be found in appendix A.

Oceanic Mixed Layer absorbs all downgoing longwave radiation (as well as incoming shortwave radiation) which passes through the atmospheric mixed layer. Emits radiation according to

$$F_0^\uparrow = B_0(0) = \sigma\left(\overline{{}^oT_m} + {}^oT_m{}'\right)^4. \tag{4.3}$$

We linearise this by writing

$$F_0^\uparrow \approx \overline{F_0^\uparrow} + D_0^\uparrow {}^oT_m{}' \tag{4.4}$$

where

$$\overline{F_0^\uparrow} = \sigma \overline{{}^oT_m}^4, \tag{4.5}$$

$$D_0^\uparrow = 4\sigma \overline{{}^oT_m}^3. \tag{4.6}$$

Atmospheric Mixed Layer absorbs all downgoing and upgoing longwave radiation. Linearised radiation is derived in Appendix A where we have defined the optical depths z_i at each interface. Radiation is written

$$F_m^\uparrow \approx \overline{F_m^\uparrow} + B_m^\uparrow {}^a\eta_m + D_m^\uparrow {}^aT_m{}' \tag{4.7}$$

$$F_m^\downarrow \approx \overline{F_m^\downarrow} + D_m^\downarrow {}^aT_m{}' \tag{4.8}$$

where

$$\overline{F_m^\uparrow} = \frac{\sigma}{2z_m^-}\int_0^{{}^aH_m} \left(\overline{{}^aT_m} - \gamma z\right)^4 e^{-\frac{{}^aH_m - z}{z_m^-}}\, dz \tag{4.9}$$

$$B_m^\uparrow = \frac{\sigma}{2z_m^-}(\overline{{}^aT_m} - \gamma {}^aH_m)^4 - \frac{\sigma}{2{z_m^-}^2}\int_0^{{}^aH_m} \left(\overline{{}^aT_m} - \gamma z\right)^4 e^{-\frac{{}^aH_m - z}{z_m^-}}\, dz \tag{4.10}$$

$$D_m^\uparrow = \frac{2\sigma}{z_m^-}\int_0^{{}^aH_m} \left(\overline{{}^aT_m} - \gamma z\right)^3 e^{-\frac{{}^aH_m - z}{z_m^-}}\, dz \tag{4.11}$$

$$\overline{F_m^\downarrow} = -\frac{\sigma}{2}\overline{{}^aT_m}^4 \tag{4.12}$$

$$D_m^\downarrow = -2\sigma\overline{{}^aT_m}^3 \tag{4.13}$$

Lower Troposphere is more complicated as partial absorption of incoming radiation and partial emission of the outgoing mixed layer radiation occurs:

$$F_1^\uparrow \approx \overline{F_1^\uparrow} + A_1^\uparrow{}^a\eta_1 + B_1^\uparrow{}^a\eta_m + D_1^\uparrow{}^aT_m{}' \tag{4.14}$$

$$F_1^\downarrow \approx \overline{F_1^\downarrow} + A_1^\downarrow{}^a\eta_1 + B_1^\downarrow{}^a\eta_m \tag{4.15}$$

where

$$\overline{F_1^\uparrow} \approx \overline{F_m^\uparrow}\tau_1^\uparrow + \frac{\sigma}{2z_1}\int_{{}^aH_m}^{{}^aH_1}({}^aT_1 - \gamma z)^4 e^{-\frac{{}^aH_1 - z}{z_1}}\,dz \tag{4.16}$$

$$A_1^\uparrow = -\frac{\overline{F_m^\uparrow}\tau_1^\uparrow}{z_1} + \frac{\sigma}{2z_1}({}^aT_1 - \gamma{}^aH_1)^4 - \frac{\sigma}{2z_1^2}\int_{{}^aH_m}^{{}^aH_1}({}^aT_1 - \gamma z)^4 e^{-\frac{{}^aH_1 - z}{z_1}}\,dz \tag{4.17}$$

$$B_1^\uparrow = \tau_1^\uparrow\left(\frac{\overline{F_m^\uparrow}}{z_1} + B_m^\uparrow - \frac{\sigma}{2z_1}({}^aT_1 - \gamma{}^aH_m)^4\right) \tag{4.18}$$

$$D_1^\uparrow = D_m^\uparrow\tau_1^\uparrow \tag{4.19}$$

$$\overline{F_1^\downarrow} = \overline{F_2^\downarrow}\tau_1^\downarrow - \frac{\sigma}{2z_m^+}\int_{{}^aH_m}^{{}^aH_1}({}^aT_1 - \gamma z)^4 e^{\frac{{}^aH_m - z}{z_m^+}}\,dz \tag{4.20}$$

$$A_1^\downarrow = \tau_1^\downarrow\left(-\frac{\overline{F_2^\downarrow}}{z_m^+} + A_2^\downarrow - \frac{\sigma}{2z_m^+}({}^aT_1 - \gamma{}^aH_1)^4\right) \tag{4.21}$$

$$B_1^\downarrow = \frac{\overline{F_2^\downarrow}\tau_1^\downarrow}{z_m^+} + \frac{\sigma}{2z_m^+}({}^aT_1 - \gamma{}^aH_m)^4 - \frac{\sigma}{2{z_m^+}^2}\int_{{}^aH_m}^{{}^aH_1}({}^aT_1 - \gamma z)^4 e^{\frac{{}^aH_m - z}{z_m^+}}\,dz \tag{4.22}$$

Upper Troposphere also has partial absorption and emission,

$$F_2^\uparrow \approx \overline{F_2^\uparrow} + A_2^\uparrow{}^a\eta_1 + B_2^\uparrow{}^a\eta_m + D_2^\uparrow{}^aT_m{}' \tag{4.23}$$

$$F_2^\downarrow \approx \overline{F_2^\downarrow} + A_2^\downarrow{}^a\eta_1 \tag{4.24}$$

where

$$\overline{F_2^\uparrow} = \overline{F_1^\uparrow}\tau_2^\uparrow + \frac{\sigma}{2z_2}\int_{{}^aH_1}^{{}^aH_T}({}^aT_2 - \gamma z)^4 e^{-\frac{{}^aH_T - z}{z_2}}\,dz \tag{4.25}$$

$$A_2^\uparrow = \tau_2^\uparrow\left(\frac{\overline{F_1^\uparrow}}{z_2} + A_1^\uparrow - \frac{\sigma}{2z_2}({}^aT_2 - \gamma{}^aH_1)^4\right) \tag{4.26}$$

$$B_2^\uparrow = B_1^\uparrow\tau_2^\uparrow \tag{4.27}$$

$$D_2^\uparrow = D_1^\uparrow\tau_2^\uparrow \tag{4.28}$$

$$\overline{F_2^\downarrow} = -\frac{\sigma}{2z_1}\int_{{}^aH_1}^{{}^aH_T}({}^aT_2 - \gamma z)^4 e^{\frac{{}^aH_1 - z}{z_1}}\,dz \tag{4.29}$$

$$A_2^\downarrow = \frac{\sigma}{2z_1}\left(-\frac{1}{z_1}\int_{{}^aH_1}^{{}^aH_T}({}^aT_2 - \gamma z)^4 e^{\frac{{}^aH_1 - z}{z_1}}\,dz + ({}^aT_2 - \gamma{}^aH_1)^4\right) \tag{4.30}$$

4.3 Sensible and latent heat flux

Sensible and latent heat flux from the oceanic to the atmospheric mixed layer is represented by

$$F_\lambda = \lambda({}^oT_m - {}^aT_m), \tag{4.31}$$

or in perturbation form

$$F_\lambda = \overline{F_\lambda} + \lambda({}^oT_m{}' - {}^aT_m{}'), \tag{4.32}$$

where

$$\overline{F_\lambda} = \lambda(\overline{{}^oT_m} - \overline{{}^aT_m}). \tag{4.33}$$

4.4 Entrainment heat flux

Layers 1 and 2 have constant (but different) potential temperatures. Therefore, the combined heat content of the two layers can only change when the interface dividing the layers changes its height. The entrainment ${}^ae_1$ therefore implies a vertical heat flux into or out of the QG layers. This heat flux is written as a double-sided flux (see McDougall and Dewar, 1998), so that in the atmosphere

$${}^aF_1^{e+} - {}^aF_1^{e-} = -{}^a\rho^aC_p{}^ae_1\Delta_1^aT, \tag{4.34}$$

where Δ_1^aT is the change in temperature across the interface and ${}^aF_1^{e+}$ (${}^aF_1^{e-}$) is the heat flux on the upper (lower) side of the interface. This allows a divergence of heat flux at the interface, but not within the layers.

In the atmosphere we assume no entrainment at the top of the domain:

$${}^aF_2^{e-} = 0. \tag{4.35}$$

Heat conservation equations in the two layers are

$${}^aF_2^{e-} + {}^aF_2^{\uparrow} = {}^aF_1^{e+} + {}^aF_2^{\downarrow} + {}^aF_1^{\uparrow}, \tag{4.36}$$

$${}^aF_1^{e-} + {}^aF_2^{\downarrow} + {}^aF_1^{\uparrow} = {}^aF_m^{e+} + {}^aF_1^{\downarrow} + {}^aF_m^{\uparrow}. \tag{4.37}$$

We can then find entrainment at the layer interface by combining these two equations;

$${}^ae_1 = \frac{{}^aF_m^{e+} + {}^aF_1^{\downarrow} + {}^aF_m^{\uparrow} - {}^aF_2^{\uparrow}}{{}^a\rho^aC_p\Delta_1^aT}. \tag{4.38}$$

At the mixed layer interface we assume that entrainment is maintained by turbulence on either side of the interface. In other words, assume

$${}^aF_m^{e+} = \overline{F_x} - \frac{{}^a\rho^aC_p{}^a\mu_1}{{}^aH_1 - {}^ah_m}, \tag{4.39}$$

$${}^aF_m^{e-} = \overline{F_x} - \frac{{}^a\rho^aC_p{}^a\mu_m}{{}^ah_m}, \tag{4.40}$$

where $\overline{F_x}$ is an export heat flux (a constant added heat flux), and

$$\frac{{}^a\mu_1}{{}^aH_1 - {}^aH_m} = \frac{{}^a\mu_m}{{}^aH_m}. \tag{4.41}$$

We linearise the above equations to give

$${}^aF_m^{e+} = \overline{F_x} - \frac{{}^a\rho^aC_p{}^a\mu_1}{{}^aH_1 - {}^aH_m}, \tag{4.42}$$

$$ {}^aF_m^{e-} = \overline{{}^aF_m^{e-}} - \frac{{}^a\rho {}^aC_p {}^a\mu_m}{{}^aH_m}\left(1 - \frac{{}^a\eta_m}{{}^aH_m}\right). \tag{4.43} $$

Then

$$ {}^ae_m \approx \frac{{}^a\phi_m}{{}^a\rho {}^aC_p \Delta_m^a T} {}^a\eta_m, \tag{4.44} $$

where

$$ {}^a\phi_m \equiv \frac{{}^a\rho {}^aC_p {}^a\mu_m}{{}^aH_m{}^2}. \tag{4.45} $$

In the model we then use the perturbation forcing

$$ {}^aF_m^{e-} = \overline{{}^aF_m^{e-}} + {}^a\phi_m {}^a\eta_m \tag{4.46} $$

$$ {}^aF_m^{e+} = \overline{{}^aF_m^{e-}}. \tag{4.47} $$

In the ocean, the heat flux at the ocean floor is zero, leaving

$$ {}^oF_2^{e+} = 0. \tag{4.48} $$

In addition we can write

$$ {}^oF_2^{e+} = {}^oF_1^{e-}, \tag{4.49} $$

since there is no heat flux gradient within layer 2, and no other source of heat there, leaving

$$ {}^oF_1^{e-} = 0. \tag{4.50} $$

From (4.34) we write

$$ {}^oF_1^{e+} = -{}^o\rho {}^oC_p {}^oe_1 \Delta_1^o T. \tag{4.51} $$

In the oceanic mixed layer, where there is no variation in mixed layer depth, entrainment is solely driven by Ekman pumping,

$$ {}^oe_m = {}^ow_{ek}. \tag{4.52} $$

Using a centred difference model for entrainment there, we find

$$ {}^oF_m^{e+} = -0.5 {}^o\rho {}^oC_p \Delta_m^o T {}^ow_{ek} \tag{4.53} $$

$$ {}^oF_m^{e-} = 0.5 {}^o\rho {}^oC_p \Delta_m^o T {}^ow_{ek} \tag{4.54} $$

Therefore we can write

$$ {}^oe_1 = -\frac{\Delta_m^o T}{2\Delta_1^o T} {}^ow_{ek} \tag{4.55} $$

5 Layer equations

We are now in a position to put together equations for each layer. A schematic of the model which includes radiative fluxes, entrainment velocities and momentum coupling is shown in figure 1.

5.1 Ocean layer 1

From (2.18) we can write

$$ {}^oq_{1t} + ({}^ou_1{}^oq_1)_x + ({}^ov_1{}^oq_1)_y = \frac{f_0}{{}^oH_1}({}^ow_{ek} - {}^oe_1) - \frac{{}^oA_H}{f_0}\nabla_H^6{}^op_1. \tag{5.1} $$

where the Ekman pumping has been explicitly included, and

$$ {}^oq_1 = \frac{\nabla_H^2{}^op_1}{f_0} + \beta y + \frac{f_0{}^o\eta_1}{{}^oH_1}. \tag{5.2} $$

Layer thickness ${}^oh_1$ is the sum of a constant and a varying part

$$ {}^oh_1 = {}^oH_1 - {}^o\eta_1, \tag{5.3} $$

and ${}^o\eta_1$ can be found from the pressure field via

$$ {}^o\eta_1 = -\frac{{}^op_1 - {}^op_2}{{}^og'}. \tag{5.4} $$

From (4.55),

$$ {}^oe_1 = -\frac{\Delta_m^oT}{2\Delta_1^oT}{}^ow_{ek}. \tag{5.5} $$

This equation will be altered if convection occurs.

5.2 Ocean layer 2

From (2.19) we can write

$$ {}^oq_{2t} + ({}^ou_2{}^oq_2)_x + ({}^ov_2{}^oq_2)_y = \frac{f_0}{{}^oH_2}({}^oe_1 - \frac{\delta_e}{2f_0}\nabla_H^2{}^op_2) - \frac{{}^oA_H}{f_0}\nabla_H^6{}^op_2. \tag{5.6} $$

where

$$ {}^oq_2 = \frac{\nabla_H^2{}^op_2}{f_0} + \beta y - \frac{f_0{}^o\eta_1}{{}^oH_2}. \tag{5.7} $$

5.3 Ocean mixed layer

From (3.21),

$$ {}^oT_{mt} + ({}^ou_m{}^oT_m)_x + ({}^ov_m{}^oT_m)_y - \frac{{}^ow_{ek}{}^oT_m}{{}^oH_m} = {}^oK_H\nabla_H^2{}^oT_m + \frac{{}^oF_0 + {}^oF_m^{e+}}{{}^o\rho{}^oC_p{}^oH_m}, \tag{5.8} $$

where total oceanic mixed layer forcing is given by

$$ {}^oF_0 = -F_\lambda - F_0^\uparrow - F_m^\downarrow - F_s, \tag{5.9} $$

and we have retained the entrainment flux as a separate term in (5.8). Note that the advective terms here use the mixed layer velocity which is modified by stress, rather than the geostrophic velocity used in (5.1) and (5.6).

5.4 Atmosphere layer 1

From (2.14) we can write

$$ {}^{a}q_{1t} + ({}^{a}u_1{}^{a}q_1)_x + ({}^{a}v_1{}^{a}q_1)_y = \frac{f_0}{{}^{a}H_1}({}^{a}e_1 - {}^{a}w_{ek}) - \frac{{}^{a}A_H}{f_0}\nabla_H^6\,{}^{a}p_1. \tag{5.10} $$

where

$$ {}^{a}q_1 = \frac{\nabla_H^2\,{}^{a}p_1}{f_0} + \beta y - \frac{f_0{}^{a}\eta_1}{{}^{a}H_1}, \tag{5.11} $$

and the interface height can be found by

$$ {}^{a}\eta_1 = \frac{{}^{a}p_1 - {}^{a}p_2}{{}^{a}g'}. \tag{5.12} $$

Interfacial flux is found via (4.38)

$$ {}^{a}e_1 = \frac{{}^{a}F_m^{e+} + F_1^{\downarrow} + F_m^{\uparrow} - F_2^{\uparrow}}{{}^{a}\rho^{a}C_p\Delta_1^{a}T}. \tag{5.13} $$

5.5 Atmosphere layer 2

From (2.14) we can write

$$ {}^{a}q_{2t} + ({}^{a}u_2{}^{a}q_2)_x + ({}^{a}v_2{}^{a}q_2)_y = -\frac{f_0}{{}^{a}H_2}{}^{a}e_1 - \frac{{}^{a}A_H}{f_0}\nabla_H^6\,{}^{a}p_2. \tag{5.14} $$

where

$$ {}^{a}q_2 = \frac{\nabla_H^2\,{}^{a}p_2}{f_0} + \beta y + \frac{f_0{}^{a}\eta_1}{{}^{a}H_2}, \tag{5.15} $$

and ${}^{a}e_1$ is given by (5.13) above.

5.6 Atmosphere mixed layer

From (3.18) and (3.20) we get

$$ {}^{a}h_{mt} + ({}^{a}u_m{}^{a}h_m)_x + ({}^{a}v_m{}^{a}h_m)_y = -{}^{a}e_m. \tag{5.16} $$

$$ {}^{a}T_{mt} + ({}^{a}u_m{}^{a}T_m)_x + ({}^{a}v_m{}^{a}T_m)_y + \frac{{}^{a}w_{ek}{}^{a}T_m}{{}^{a}H_m} = {}^{a}K_H\nabla_H^2\,{}^{a}T_m - {}^{a}K_4\nabla_H^4\,{}^{a}T_m + \frac{-{}^{a}F_m + {}^{a}F_0}{{}^{a}\rho^{a}C_p{}^{a}h_m}, \tag{5.17} $$

where atmospheric mixed layer forcing above and below the mixed layer are respectively given by

$$ {}^{a}F_m = F_m^{\uparrow} + F_1^{\downarrow} + {}^{a}F_m^{e-} \tag{5.18} $$

$$ {}^{a}F_0 = \begin{cases} F_m^{\downarrow} + F_\lambda + F_0^{\uparrow} & \text{over ocean,} \\ -F_s' & \text{over land.} \end{cases} \tag{5.19} $$

5.7 Convection

Convection will occur when unstable stratification forms and will act to change temperature in the mixed layers in a way which conserves heat. In the atmosphere, when ${}^{a}T_m$ exceeds ${}^{a}T_1$ we adjust the layer 1 entrainment as follows,

$$ \delta^{a}e_1 = \frac{{}^{a}h_m({}^{a}T_1 - {}^{a}T_m)}{2\Delta t_a\Delta_1^{a}T}, \tag{5.20} $$

and set ${}^{a}T_m = {}^{a}T_1$. Likewise, in the ocean, when ${}^{o}T_m < {}^{o}T_1$ we alter layer 1 entrainment by

$$ \delta^{o}e_1 = \frac{-{}^{o}H_m({}^{o}T_1 - {}^{o}T_m)}{2\Delta t_o\Delta_1^{o}T}, \tag{5.21} $$

and set ${}^{o}T_m = {}^{o}T_1$.

6 Mean state

The mean state is defined by the solution of the above equations when $F_s = \overline{F_s}$. In this state there will be no motion, so that pressure gradients, vorticity gradients and entrainment disappear. Our full equation set then reduces to a radiation balance between the atmosphere and the oceanic mixed layer. From (5.13) we get a heat balance in the upper atmosphere

$$\overline{{}^aF_m^{e+}} + \overline{F_1^{\downarrow}} + \overline{F_m^{\uparrow}} - \overline{F_2^{\uparrow}} = 0, \tag{6.1}$$

(5.17) gives us the heat balance in the atmospheric mixed layer

$$-\overline{F_m^{\uparrow}} - \overline{F_1^{\downarrow}} - \overline{{}^aF_m^{e-}} + [\overline{F_m^{\downarrow}} + \overline{F_\lambda} + \overline{F_0^{\uparrow}}] = 0, \tag{6.2}$$

and (5.8) can be used for the heat balance in the ocean mixed layer,

$$-\overline{F_\lambda} - \overline{F_0^{\uparrow}} - \overline{F_m^{\downarrow}} - \overline{F_s} + \overline{{}^oF_m^{e+}} = 0, \tag{6.3}$$

where ${}^oF_m^{e+} = 0$ and ${}^ae_m = 0$. These equations can be manipulated to write

$$\overline{F_2^{\uparrow}} = -\overline{F_s}, \tag{6.4}$$

which yields $\overline{{}^aT_m}$ provided one has knowledge of temperature, transmissivity and layer height in the atmosphere. Equation (6.3) can be written as a quartic equation in $\overline{{}^oT_m}$ to give oceanic mixed layer temperature. The value of ${}^a\mu_m$ (and hence ${}^a\mu_1$) are prescribed, and export heat fluxes are adjusted to satisfy (6.2).

7 Final equation set

The full set of equations for the two layer version is now written in the order in which they are solved in the model. The equation numbers used here are referred to in comments in the code. Specified parameters are shown in Tables 1 and 2, along with derived radiation coefficients in Table 3.

At the start of each ocean timestep we find the atmospheric stress from (3.3), (3.5a) and (3.5b):

$$({}^a\tau^x, {}^a\tau^y) = \frac{C_D|\mathbf{{}^au_m}|}{\chi}\left({}^au_1 - \frac{C_D|\mathbf{{}^au_m}|}{{}^aH_m f_0}{}^av_1, {}^av_1 - \frac{C_D|\mathbf{{}^au_m}|}{{}^aH_m f_0}{}^au_1\right), \tag{7.1}$$

where

$$({}^au_1, {}^av_1) = \frac{1}{f_0}\left(-{}^ap_{1y}, {}^ap_{1x}\right), \tag{7.2}$$

$$|\mathbf{{}^au_m}| = \frac{\sqrt{2}\,C_D}{{}^aH_m f_0}\sqrt{-1 + \sqrt{1 + 4\left(\frac{C_D}{{}^aH_m f_0}\right)^2}}, \tag{7.3}$$

and

$$\chi \equiv 1 + \left(\frac{C_D|\mathbf{{}^au_m}|}{{}^aH_m f_0}\right)^2. \tag{7.4}$$

We use this to find the ocean stress from (3.9)

$${}^o\tau = \xi\frac{{}^a\rho}{{}^o\rho}{}^a\tau, \tag{7.5}$$

Parameters	Value	Description
$(^aX, ^aY)$	(15360, 7920) km	Domain size
$(^aH_1, ^aH_2)$	(4000, 6000) m	Layer heights
^aH_m	1000 m	Mean mixed layer height
$(^aT_1, ^aT_2)$	(330, 350) K	Potential temperature structure
Δx_a	120 km	Horizontal grid spacing
Δt_a	5 min	Timestep
$^a\rho$	1 kg/m^3	Density
^aC_p	1000 J/kg/K	Specific heat capacity
$^ag'$	2 m/s^2	Reduced gravity
C_D	1.6×10^{-3}	Drag coefficient
^aA_H	2×10^{14} m^4/s	Horizontal viscosity coefficient
$^a\alpha$	10	Mixed boundary condition coefficient
^aK_H	2.7×10^4 m^2/s	Horizontal temperature diffusion coefficient
$^aK_4$	3×10^{14} m^4/s	Horizontal 4th order diffusion coefficient
K_η	8×10^4 m^2/s	Horizontal diffusion coefficient for $^a\eta_m$
$^a\phi_m$	0.08 W/m^3	Relaxation rate for mixed layer height
σ	5.6704×10^{-8} W/m^2/K^4	Stefan–Boltzmann constant
γ	0.01 K/m	Adiabatic lapse rate
$\overline{F_s}$	-210 W/m^2	Mean incoming radiation
$\lvert F'_s \rvert$	75 W/m^2	Amplitude of variable incoming radiation
λ	35 W/m^2/K	Sensible and latent heat flux coefficient
z_0	0 m	Optical depth at the base of the mixed layer
z_m^-	200 m	Optical depth just below the M. L. interface
z_m^+	30 000 m	Optical depth just above the M. L. interface
z_1	20 000 m	Optical depth in layer 1
z_2	40 000 m	Optical depth in layer 2

Table 1: Specified default atmospheric parameters for Q-GCM.

Parameters	Value	Description
$(^oX, ^oY)$	(3840, 6000) km	Domain size
$(^oH_1, ^oH_2)$	(1000, 3000) m	Layer heights
^oH_m	100 m	Mixed layer height (fixed)
$(^oT_1, ^oT_2)$	(278, 268) K	Potential temperature structure
Δx_o	15 km	Horizontal grid spacing
Δt_o	45 min	Timestep
$^o\rho$	1000 kg/m^3	Density
^oC_p	4000 J/kg/K	Specific heat capacity
$^og'$	0.02 m/s^2	Reduced gravity
δ_e	1 m	Bottom Ekman layer thickness
^oA_H	2.0×10^{10} m^4/s	Horizontal viscosity coefficient
$^o\alpha$	0	Mixed boundary condition coefficient (free slip)
^oK_H	200 m^2/s	Horizontal temperature diffusion coefficient
f_0	1×10^{-4} s^{-1}	Mean Coriolis parameter
β	2×10^{-11} (ms)$^{-1}$	Coriolis parameter gradient
ξ	1.0	Atmosphere–ocean stress multiplier

Table 2: Specified default oceanic parameters for Q-GCM.

Parameters	Value	Description
$\overline{F_0^{\uparrow}}$	468.5 W/m^2	Mean upward flux from surface
$\overline{F_m^{\downarrow}}$	-236.2 W/m^2	Mean downward flux from mixed layer
$\overline{F_m^{\uparrow}}$	210.6 W/m^2	Mean upward flux from surface
$\overline{F_1^{\downarrow}}$	-66.2 W/m^2	Mean downward flux from layer 1
$\overline{F_1^{\uparrow}}$	215.4 W/m^2	Mean upward flux from layer 1
$\overline{F_2^{\downarrow}}$	-47.2 W/m^2	Mean downward flux from layer 2
$\overline{F_2^{\uparrow}}$	210 W/m^2	Mean outgoing flux
$A_1^{\downarrow}$	5.09 $\times 10^{-3}$ W/m^3	Perturbation to downward layer 1 radiation (${}^a\eta_1$)
$A_1^{\uparrow}$	-7.46 $\times 10^{-4}$ W/m^3	Perturbation to upward layer 1 radiation (${}^a\eta_1$)
$A_2^{\downarrow}$	1.07 $\times 10^{-2}$ W/m^3	Perturbation to downward layer 2 radiation (${}^a\eta_1$)
$A_2^{\uparrow}$	-1.64 $\times 10^{-3}$ W/m^3	Perturbation to outgoing radiation (${}^a\eta_1$)
$B_m^{\uparrow}$	-2.07 $\times 10^{-2}$ W/m^3	Perturbation to upward mixed layer radiation (${}^a\eta_m$)
$B_1^{\downarrow}$	7.70 $\times 10^{-3}$ W/m^3	Perturbation to downward layer 1 radiation (${}^a\eta_m$)
$B_1^{\uparrow}$	-1.74 $\times 10^{-2}$ W/m^3	Perturbation to upward layer 1 radiation (${}^a\eta_m$)
$B_2^{\uparrow}$	-1.50 $\times 10^{-2}$ W/m^3	Perturbation to outgoing radiation (${}^a\eta_m$)
$D_0^{\uparrow}$	6.22 W/m^2/K	Perturbation to upward surface radiation (${}^oT_m{}'$)
$D_m^{\downarrow}$	-3.13 W/m^2/K	Perturbation to downward mixed layer radiation (${}^aT_m{}'$)
$D_m^{\uparrow}$	2.86 W/m^2/K	Perturbation to upward mixed layer radiation (${}^aT_m{}'$)
$D_1^{\uparrow}$	2.47 W/m^2/K	Perturbation to upward layer 1 radiation (${}^aT_m{}'$)
$D_2^{\uparrow}$	2.12 W/m^2/K	Perturbation to outgoing radiation (${}^aT_m{}'$)
${}^oT_S$	29.6 K	Derived relative Southern boundary temperature

Table 3: Default derived radiation parameters for Q-GCM. Perturbation coefficients include (in brackets) the variable by which they are multiplied to produce heat flux.

which requires interpolating stress onto the oceanic pressure grid and multiplication by the constant ${}^a\rho/{}^o\rho$. The Ekman velocities can then be calculated (on the temperature grid, and then averaged onto the pressure grid) from (3.8) and (3.10)

$$ {}^aw_{ek} = \frac{1}{f_0}({}^a\tau_x^y - {}^a\tau_y^x), \tag{7.6} $$

$$ {}^ow_{ek} = \frac{1}{f_0}({}^o\tau_x^y - {}^o\tau_y^x). \tag{7.7} $$

The radiative flux at the atmospheric mixed layer boundaries is determined at this stage from (5.17)

$$ {}^aF_m = A_1^{\downarrow}{}^a\eta_1 + ({}^a\phi_m + B_m^{\uparrow} + B_1^{\downarrow}){}^a\eta_m + D_m^{\uparrow}\,{}^aT_m{}', \tag{7.8} $$

$$ {}^aF_0 = \begin{cases} D_m^{\downarrow}\,{}^aT_m{}' + D_0^{\uparrow}\,{}^oT_m{}' + \lambda({}^oT_m{}' - {}^aT_m{}') & \text{over ocean,} \\ -F_s' & \text{over land.} \end{cases} \tag{7.9} $$

In the ocean,

$$ {}^oF_0 = D_m^{\downarrow}\,{}^aT_m{}' + D_0^{\uparrow}\,{}^oT_m{}' + \lambda({}^oT_m{}' - {}^aT_m{}') + F_s'. \tag{7.10} $$

The next stage is to determine the evolution of the oceanic mixed layer using (5.8),

$$ {}^oT_{mt}{}' = -({}^ou_m{}^oT_m{}')_x - ({}^ov_m{}^oT_m{}')_y + \frac{{}^ow_{ek}({}^oT_1 + {}^oT_m{}')}{2{}^oH_m} + {}^oK_H\nabla_H^2\,{}^oT_m{}' - \frac{{}^oF_0}{{}^o\rho{}^oC_p{}^oH_m}. \tag{7.11} $$

This involves integrating forward in time. Note here that oceanic layer temperatures are defined relative to $\overline{{}^oT_m}$ so that terms including the mean temperature disappear. The entrainment at the interface between layers 1 and 2 is written from (5.5) as,

$$ {}^oe_1 = -\frac{\Delta_m^o T}{2\Delta_1^o T}{}^ow_{ek} \tag{7.12} $$

After timestepping (7.11), if ${}^oT_m < {}^oT_1$, convection will occur. This requires a correction to the interfacial entrainment which is handled by adding

$$ \delta^o e_1 = \frac{-{}^oH_m({}^oT_1 - {}^oT_m)}{2\Delta t_o \Delta_1^o T} \tag{7.13} $$

to the existing entrainment ${}^oe_1$. We then correct mixed layer temperature by setting ${}^oT_m = {}^oT_1$.

Next we are in a position to step the QG equations in all parts of the domain except for the boundaries. Do this by recasting (5.1) and (5.6)

$$ {}^oq_{1t} = \frac{f_0}{{}^oH_1}({}^ow_{ek} - {}^oe_1) - ({}^ou_1{}^oq_1)_x - ({}^ov_1{}^oq_1)_y - \frac{{}^oA_H}{f_0}\nabla_H^6{}^op_1, \tag{7.14} $$

$$ {}^oq_{2t} = \frac{f_0}{{}^oH_2}{}^oe_1 - \frac{\delta_e}{2{}^oH_2}\nabla_H^2{}^op_2 - ({}^ou_2{}^oq_2)_x - ({}^ov_2{}^oq_2)_y - \frac{{}^oA_H}{f_0}\nabla_H^6{}^op_2. \tag{7.15} $$

Note that the vorticity equation does not apply on boundary points, and the boundary conditions we use are formulated in terms of pressure. Pressure is determined by writing the barotropic and baroclinic vorticities respectively as

$$ f_0({}^oH_1{}^oq_1 + {}^oH_2{}^oq_2 - ({}^oH_1 + {}^oH_2)\beta y) = \nabla_H^2({}^oH_1{}^op_1 + {}^oH_2{}^op_2), \tag{7.16} $$

$$ f_0({}^oq_1 - {}^oq_2) = (\nabla_H^2 - {}^or_d{}^{-2})({}^op_1 - {}^op_2), \tag{7.17} $$

where $r_d \equiv \sqrt{\frac{H_1H_2{}^og'}{f_0^2(H_1+H_2)}}$ is the radius of deformation. Since the left hand side of these two equations are known, the barotropic and baroclinic pressure fields are found using a Helmholtz solver (see §8.3 for details). It is at this time that the mass constraint is included (see Appendix B.1). Layer pressures are recovered by writing

$$ \frac{1}{{}^oH_1 + {}^oH_2}({}^oH_1{}^op_1 + {}^oH_2{}^op_2 - {}^oH_1({}^op_1 - {}^op_2)) = {}^op_2, \tag{7.18} $$

$$ {}^op_2 + ({}^op_1 - {}^op_2) = {}^op_1. \tag{7.19} $$

Boundary values of vorticity are recovered from the pressure field using boundary constraints (see Appendix C).

We are then ready to timestep the atmosphere internal points. As in the ocean case we begin by recalculating (7.6) on the temperature grid, and from (5.16) and (5.17) we get

$$ {}^ah_{mt} = -({}^au_m{}^ah_m)_x - ({}^av_m{}^ah_m)_y + K_\eta\nabla_H^2{}^ah_m - \frac{{}^a\phi_m{}^a\eta_m}{{}^a\rho^aC_p\Delta_m^aT}, \tag{7.20} $$

where an extra diffusive term has been added for numerical stability, and

$$ {}^aT_{mt}' = -({}^au_m{}^aT_m')_x - ({}^av_m{}^aT_m')_y - \frac{{}^aw_{ek}{}^aT_m'}{{}^aH_m} + {}^aK_H\nabla_H^2{}^aT_m' - {}^aK_4\nabla_H^4{}^aT_m' + \frac{-{}^aF_m + {}^aF_0}{{}^a\rho^aC_p{}^ah_m}. \tag{7.21} $$

Entrainment at the top of layer 1 in the atmosphere is found using (5.13),

$$ {}^ae_1 = \frac{(A_1^\downarrow - A_2^\uparrow)^a\eta_1 + (B_1^\downarrow + B_m^\uparrow - B_2^\uparrow)^a\eta_m + (D_m^\uparrow - D_2^\uparrow)^aT_m'}{{}^a\rho^aC_p\Delta_1^aT}. \tag{7.22} $$

Convection will occur when, after timestepping ${}^aT_m{}' > {}^aT_1$, in which case we adjust the entrainment at the top of layer 1 by adding

$$\delta^a e_1 = \frac{{}^a h_m({}^aT_1 - {}^aT_m)}{2\Delta t_a \Delta_1^a T} \tag{7.23}$$

and then set the temperature to be ${}^aT_m{}' = {}^aT_1$.

Finally we step the atmosphere QG equations by writing (5.10) and (5.14) as

$${}^a q_{1t} = \frac{f_0}{{}^aH_1}({}^ae_1 - {}^aw_{ek}) - ({}^au_1{}^aq_1)_x - ({}^av_1{}^aq_1)_y - \frac{{}^aA_H}{f_0}\nabla_H^6\, {}^ap_1, \tag{7.24}$$

$${}^a q_{2t} = -\frac{f_0}{{}^aH_2}{}^ae_1 - ({}^au_2{}^aq_2)_x - ({}^av_2{}^aq_2)_y - \frac{{}^aA_H}{f_0}\nabla_H^6\, {}^ap_2. \tag{7.25}$$

As before, the pressures are easiest to find in modal form which are determined as follows,

$$f_0({}^aH_1{}^aq_1 + {}^aH_2{}^aq_2 - ({}^aH_1 + {}^aH_2)\beta y) = \nabla_H^2({}^aH_1{}^ap_1 + {}^aH_2{}^ap_2), \tag{7.26}$$

$$f_0({}^aq_1 - {}^aq_2) = (\nabla_H^2 - {}^ar_d{}^{-2})({}^ap_1 - {}^ap_2). \tag{7.27}$$

Again, pressures are found using a Helmholtz solver, and the momentum conditions described Appendix B.2 are applied. Layer pressures are recovered from modal pressures using the same formulation as for the ocean in (7.18) and (7.19) and boundary values of vorticity found from the pressure field.

8 Numerical formulation

Having derived the continuous equations which are the basis of the model, we must now formulate finite approximations to them in order to produce a computable solution. This chapter gives a brief account of the numerical methods used.

8.1 Discretisation in space and time

The domains are constructed so that (in the current version) there are 8 ocean gridlengths within each atmosphere gridlength, and the ocean occupies an integral number of atmosphere gridlengths (see figure 2). The other major difference between the atmosphere and ocean is that atmospheric velocities are much higher, and therefore, despite the larger grid cells, the atmosphere requires a smaller timestep. In this version of the model there are 9 atmosphere time steps within each ocean timestep. To conserve heat and momentum, forcing terms cannot be re-computed every atmosphere timestep: instead these terms are computed before each ocean timestep, and are held constant during the 9 atmosphere timesteps.

Both atmosphere and ocean variables are discretised horizontally on an Arakawa C-grid (Arakawa and Lamb, 1977) as shown in figure 2. The grid is Cartesian, with the same resolution in both x- and y-directions. Pressure and vorticity are tabulated at the same points (referred to consistently as p points), and temperature and mixed layer thickness are tabulated at the temperature (T) points. These are the prognostic fields; other quantities can be diagnosed from them at the appropriate gridpoints as required. When it is necessary to interpolate quantities from the coarse atmospheric grid to the finer oceanic grid, we use a simple and efficient bilinear interpolation scheme which is conservative.

The advective terms in mixed layer evolution equations such as (7.11), (7.20) and (7.21) are formulated in the usual manner for C-grid models, in which the advective velocities are computed at the centres of the faces of the cell containing a T gridpoint. This ensures that the advection scheme is conservative, and that unlike some more sophisticated advection

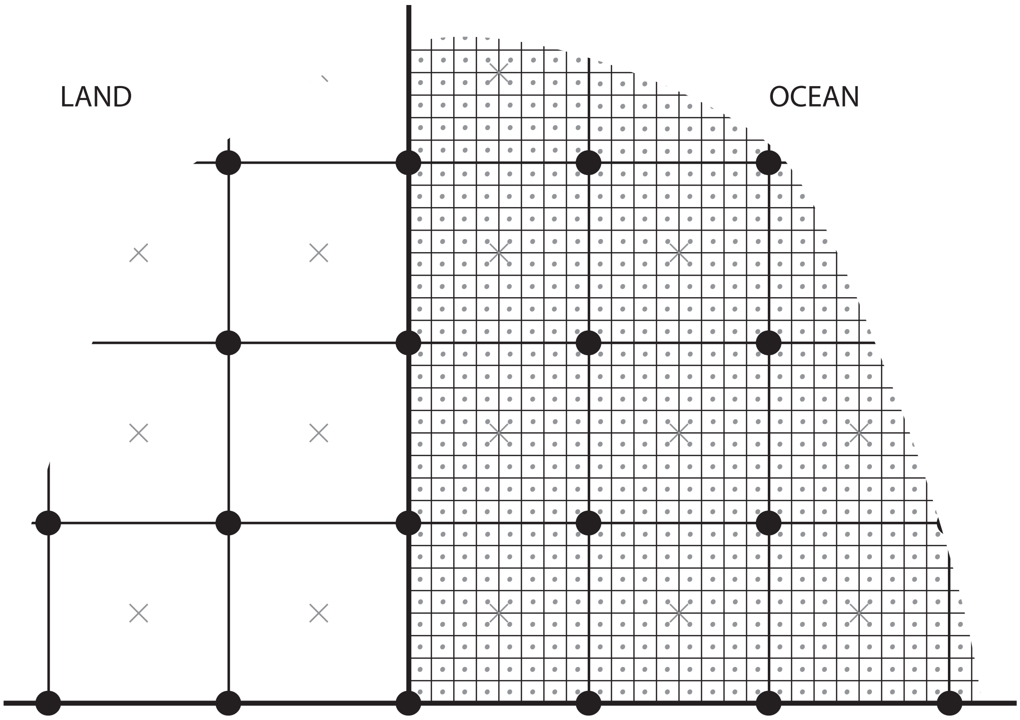

Figure 2: Cutaway section showing the grid used in the implementation of the model near the land-ocean boundary. The atmosphere grid is the larger grid, with • showing the pressure grid points and × showing the temperature gridpoints. The ocean grid is also shown, with eight ocean gridlengths to every atmosphere gridlength. The ocean pressure gridpoints are at the vertices of the grid shown, and ocean temperature points indicated by ·.

schemes there is no implicit diffusion; it is all explicit. The quantity being advected is approximated by the average of its values on either side of the face.

The exception to this is the advection of vorticity in equations (7.14 – 7.15) and (7.24 – 7.25). Here we use a higher order Arakawa Jacobian (Arakawa and Lamb, 1981) with superior conservation properties: it conserves both energy and enstrophy.

The timestepping of the evolution equations uses a leapfrog scheme, which is second order in time. Occasional averaging of the two time levels carried by the program is performed, to suppress the computational mode which is inevitable with this scheme.

8.2 Effect of the Laplacian operator on a Fourier component

This section considers the effect of the $\frac{\partial^2}{\partial x^2}$ operator on a single Fourier component; the results will prove useful in a couple of later sections. Consider a one-dimensional Fourier expansion (the extension to two dimensions is straightforward):

$$p(x) = \sum_k \tilde{p}_k e^{2\pi i k x}. \tag{8.1}$$

In the continuous case, applying the second derivative operator gives

$$\frac{d^2 p}{dx^2} = \sum_k -\tilde{p}_k (2\pi k)^2 e^{2\pi i k x}. \tag{8.2}$$

In the finite difference case, $\frac{d^2p}{dx^2}$ at x is given by the centred-difference approximation

$$\frac{d^2p}{dx^2} = \frac{p(x+dx) - 2p(x) + p(x-dx)}{dx^2}. \tag{8.3}$$

where dx is the gridspacing. Substituting (8.1) and simplifying somewhat gives

$$\frac{d^2p}{dx^2} = \sum_k \tilde{p}_k \left(\frac{e^{2\pi ikdx} + e^{-2\pi ikdx} - 2}{dx^2} \right) e^{2\pi ikx}, \tag{8.4}$$

i.e.

$$\frac{d^2p}{dx^2} = \sum_k \tilde{p}_k \left(\frac{2cos(2\pi kdx) - 2}{dx^2} \right) e^{2\pi ikx}, \tag{8.5}$$

which, using some familiar trigonometric identities, reduces to:

$$\frac{d^2p}{dx^2} = \sum_k -\tilde{p}_k \left(\frac{2sin(\pi kdx)}{dx} \right)^2 e^{2\pi ikx}. \tag{8.6}$$

So the finite difference result (8.6) is similar to the continuous result (8.2), but with the replacement

$$\pi k \Rightarrow \frac{sin(\pi kdx)}{dx}, \tag{8.7}$$

in the Fourier coefficient. For small k (well-resolved wavelengths) these are equivalent.

8.3 Solution of the Helmholtz equation

Most of the equations which constitute the model define one variable explicitly in terms of other variables or their derivatives. The exceptions are the Helmholtz equations (7.16 – 7.17) and (7.26 – 7.27) which define pressures *implicitly* in terms of vorticities, subject to suitable boundary conditions. We require a computationally efficient solution method for such equations. Write the general inhomogeneous Helmholtz equation as

$$\left(\nabla^2 - \frac{1}{r_d^2} \right) p = R \tag{8.8}$$

where the right hand side $R(x, y)$ is a known function and r_d is the Rossby radius for a given mode. The barotropic mode is a special case for which r_d is infinite, and (8.8) reduces to Poisson's equation.

We will consider the solution to (8.8) in a channel periodic in x (the atmospheric case). The method carries over to the finite ocean box with simple modifications to be discussed later. Assume the pressure $p(x, y)$ and the right hand side $R(x, y)$ are tabulated on a regular grid at positions $x_i = (i-1)dx$ (M points), $y_j = y_0 + (j-1)dy$ (N points), so that R is an $M \times N$ matrix R_{ij}. Expand p and R as a one-dimensional Fourier series in the x-direction at each of the $(N-2)$ values y_j within the domain (i.e. not including the zonal boundaries $j = 1$ and $j = N$):

$$p_{ij} = \sum_k \tilde{p}_{k,j} e^{2\pi ikx_i}. \tag{8.9}$$

We can use a Fast Fourier Transform (FFT) routine to efficiently compute the array of coefficients $\tilde{R}_{k,j}$ from the known R_{ij}. The particular ordering of the values of k in the transform vector depends on the FFT package used, so we ignore such details in this general account.

Then from (8.6)

$$\frac{\partial^2 p_{ij}}{\partial x^2} = \sum_k -\tilde{p}_{k,j}\left(\frac{2sin(\pi k dx)}{dx}\right)^2 e^{2\pi i k x_i}. \tag{8.10}$$

$\frac{\partial^2 p_{ij}}{\partial y^2}$ at $y = y_j$ is given by the usual centred difference approximation (8.3)

$$\frac{d^2 p_{ij}}{dy^2} = \sum_k \left(\frac{\tilde{p}_{k,j+1} - 2\tilde{p}_{k,j} + \tilde{p}_{k,j-1}}{dy^2}\right) e^{2\pi i k x_i} \tag{8.11}$$

so at each internal point i, j we have an equation of the form

$$\sum_k -\tilde{p}_{k,j}\left(\left(\frac{2sin(\pi k dx)}{dx}\right)^2 + \frac{1}{r_d^2}\right) e^{2\pi i k x_i} + \sum_k \left(\frac{\tilde{p}_{k,j+1} - 2\tilde{p}_{k,j} + \tilde{p}_{k,j-1}}{dy^2}\right) e^{2\pi i k x_i} = \sum_k \tilde{R}_{k,j} e^{2\pi i k x_i}. \tag{8.12}$$

But for this to be true for at all the points $x = x_i$, it must be true for each Fourier component $e^{2\pi i k x}$ separately, i.e. for all k and j, we must have

$$-\tilde{p}_{k,j}\left(\left(\frac{2sin(\pi k dx)}{dx}\right)^2 + \frac{1}{r_d^2}\right) + \frac{(\tilde{p}_{k,j+1} - 2\tilde{p}_{k,j} + \tilde{p}_{k,j-1})}{dy^2} = \tilde{R}_{k,j}. \tag{8.13}$$

For each value of the M values of k, we can thus write the set of $(N-2)$ equations (8.13) for the range of internal j values as a single tridiagonal matrix equation of size $(N-2) \times (N-2)$ relating the unknown vector $\tilde{p}_{k,j}$ and the known vector $\tilde{R}_{k,j}$:

$$\begin{bmatrix} \cdot & \cdot & & & & & & & & & \\ \cdot & \cdot & \cdot & & & & & & & & \\ & \cdot & \cdot & \cdot & & & & & & & \\ & & \cdot & \cdot & \cdot & & & & & & \\ & & & & & & & & & & \\ & & & a & b_k & a & & & & & \\ & & & & a & b_k & a & & & & \\ & & & & & a & b_k & a & & & \\ & & & & & & & & & & \\ & & & & & & \cdot & \cdot & \cdot & & \\ & & & & & & & \cdot & \cdot & \cdot & \\ & & & & & & & & \cdot & \cdot & \cdot \\ & & & & & & & & & \cdot & \cdot \end{bmatrix} \tilde{p}_{k,j} = \tilde{R}_{k,j} \tag{8.14}$$

where dots denote non-zero coefficients, and the a and b coefficients are known:

$$a = \frac{1}{dy^2}, \tag{8.15}$$

$$b_k = -\left(\left(\frac{2sin(\pi k dx)}{dx}\right)^2 + \frac{1}{r_d^2}\right) - 2a \tag{8.16}$$

Note that to maintain strictly tridiagonal form, only two entries appear on the top and bottom rows of the matrix. This is equivalent to asserting that $\tilde{p}$ vanishes on the zonal boundaries $j = 1$ and $j = N$ for all k, and thus $p = 0$ also.

Such a tridiagonal system can be efficiently solved for the unknown vector without a full matrix inversion; see any good numerical linear algebra textbook, such as Press et al. (1992). For the Helmholtz operator, it is clear from (8.16) that $|b_k| \geq 2|a|$ for all k, so the matrix is "diagonally dominant", and no problems of zero pivots can occur. The tridiagonal solution method is built into the subroutines `chsolv` and `solb`. Having solved the system for $\tilde{p}_{k,j}$ at all M wavenumbers k, we can then use (8.9) at each latitude to get the pressure p_{ij} at all gridpoints. Thus we have solved the inhomogeneous Helmholtz equation (8.8) in a zonally periodic channel, subject to the condition $p = 0$ on the zonal boundaries.

For the ocean, where we require p to be constant around the entire boundary, we use Fourier sine transforms instead of the periodic Fourier transforms, to ensure that $p = 0$ on the meridional boundaries too.

Note that the various Fourier transform routines use a significant fraction of the total CPU time (12%–18% for the default case, depending on the computer system used). It is therefore important that the parameters determining the transform lengths (`nxa`, `ndxr` and `nxaooc`, all set in `parameter.src`) should be chosen to have numerous small prime factors, so as to maximise the efficiency of the transform routines.

We can also use this scheme to solve the homogeneous Helmholtz equation for baroclinic modes. The homogeneous equation is:

$$\left(\nabla^2 - \frac{1}{r_d^2}\right) p = 0. \tag{8.17}$$

Write $p = \mathcal{L} + s$, where $\mathcal{L}$ is a known solution of Laplace's equation $\nabla^2\mathcal{L} = 0$ which is non-zero on the boundaries; then s satisfies

$$\left(\nabla^2 - \frac{1}{r_d^2}\right) s = \frac{\mathcal{L}}{r_d^2}, \tag{8.18}$$

which is of the same form as (8.8). s satisfies the usual condition $s = 0$ on the solid boundaries of the domain, so $p = \mathcal{L}$ on these boundaries. We can add any multiple of these homogeneous solutions to the inhomogeneous solution to obtain any required value of p on the solid boundaries.

8.4 Integration routines

Several of the radiative flux coefficients introduced in section 8.2 involve vertical integrals over the appropriate layers. A subroutine `trapin` is provided which computes the extended trapezoidal rule approximation to the integral of a tabulated function (Press et al., 1992). Two routines, `xintt` and `xintp`, are provided for computing area integrals. `xintt` computes the area integral of a quantity tabulated at T points, as a simple sum. `xintp` computes the area integral of a quantity tabulated at p points, as a simple sum over interior values, with an additional factor controlling the contribution of edge values to the integral.

8.5 Diffusive timescales

Several of the equations contain diffusive terms of second or fourth order (recall that the ∇^6 terms in (7.14 – 7.15) and (7.24 – 7.25) were originally introduced as fourth order terms in (2.7a,b), and are effectively fourth order since $q \sim \nabla^2 p$). To understand the damping effect of the diffusion coefficients, it is useful to derive their associated timescales.

Consider some field $p(x, y)$, and introduce second and fourth order diffusive terms into its evolution equation, with coefficients A_2 and A_4 respectively, so that

$$\frac{\partial p}{\partial t} = \ldots + A_2\nabla^2 p - A_4\nabla^4 p. \tag{8.19}$$

We will require $A_2, A_4 > 0$ to ensure decay. Expand p as a two-dimensional Fourier transform:

$$p(x,y) = \sum_k \sum_l \tilde{p}_{kl} e^{2\pi i(kx+ly)} \tag{8.20}$$

then, differentiating the Fourier expansion, we find that each term will cause exponential decay of the coefficient $\tilde{p}_{kl}$, with timescales τ_2, τ_4 given in the finite difference case (using (8.6)) by

$$\frac{1}{\tau_2} = A_2 \left(\left(\frac{2sin(\pi k\delta)}{\delta} \right)^2 + \left(\frac{2sin(\pi l\delta)}{\delta} \right)^2 \right) \tag{8.21}$$

$$\frac{1}{\tau_4} = A_4 \left(\left(\frac{2sin(\pi k\delta)}{\delta} \right)^2 + \left(\frac{2sin(\pi l\delta)}{\delta} \right)^2 \right)^2 , \tag{8.22}$$

where δ is the (equal) gridlength in either direction. The main program evaluates these timescales for two special cases:

1. A circular eddy whose radius is the baroclinic Rossby radius r_d, so $k = l = \frac{1}{2r_d}$,

$$\frac{1}{\tau_2} = 2A_2 \left(\frac{2sin(\pi\delta/2r_d)}{\delta} \right)^2 \tag{8.23}$$

$$\frac{1}{\tau_4} = 4A_4 \left(\frac{2sin(\pi\delta/2r_d)}{\delta} \right)^4 \tag{8.24}$$

2. A one-dimensional wave at the highest wavenumber representable on the grid (two gridpoint noise), $k = \frac{1}{2\delta}$, $l = 0$

$$\frac{1}{\tau_2} = A_2 \left(\frac{2}{\delta} \right)^2 \tag{8.25}$$

$$\frac{1}{\tau_4} = A_4 \left(\frac{2}{\delta} \right)^4 \tag{8.26}$$

9 Users' guide

Having briefly described the numerical formulation of the model, we now discuss the practicalities of using the code. The code is available in gzipped tar format, which expands to a single directory.

9.1 Components of the code

The code for Q-GCM consists of a number of Fortran77 source files (`*.f`), various common block files (`*.cmn`), a file called `parameter.src` and a generic `Makefile`. The code uses two public domain software packages:

FFTPACK This is a free, portable library of Fortran routines for computing 1-D fast Fourier transforms, originally written by Paul N. Swarztrauber of NCAR, Boulder. There is an FFTPACK webpage at NCAR:
`http://www.scd.ucar.edu/softlib/FFTPACK.html`
but the package is also distributed as part of the Netlib software repository:
`http://www.netlib.org/`
in Tennessee, USA, and its various mirror sites, which include:

http://www.mirror.ac.uk/sites/netlib.bell-labs.com/netlib/ (UK)
http://netlib.uow.edu.au/ (Australia).

We use the double precision version of the library, which can usually be found in the subdirectory `bihar`. Alternatively we also distribute our own versions of the necessary routines, modified to remove some programming constructs such as "computed GOTOs" which are deprecated in Fortran90, and which cause compiler warnings (directory `mybihar`). The FFTPACK routines are included via the file `fftpack.f` which you will have to edit to point to the location of these files on your system.

netCDF available from
http://www.unidata.ucar.edu/packages/netcdf/
NetCDF (network Common Data Format) is a machine-independent, self-documenting format for representing scientific data, and a library of routines for reading and writing data in this format. You will need to have installed the netCDF libraries on your system, and to edit the `Makefile` to indicate where they are. A version of the include file `netcdf.inc` (edited to eliminate some compiler warnings) is included in the Q-CGM distribution. Our development and testing has used version 3.5.0 of netCDF.

It is our policy to use public domain packages where possible, so that anyone may use Q-GCM without having to pay for package licences.

There are several easy ways to access the data in netCDF format. One way to view the data is with the browser package ncview:
http://www.gfdl.gov/~jps/GFDL_VG_2DPackages.html.
We also use the NetCDF toolbox for Matlab :
http://woodshole.er.usgs.gov/staffpages/cdenham/public_html.

9.2 Compiling the code

The `Makefile` will take care of most of the compiling, but it contains a few flags in the `Makefile` specific to your system which must be set before it will work:

atmos_only, ocean_only Flags which, if set, restrict the model to run in atmosphere/ocean only mode. At most one of these flags should be set.

use_netcdf Flag to make use of the netCDF output facility (see below). Turn this flag off to run the model without netCDF output.

FC The command which invokes your Fortran compiler (e.g. `f77`, `g77`, `ifc`)

FFLAGS List of flags for your Fortran compiler (to control optimization/debugging/profiling etc.)

NCDIR The top directory of your netCDF installation

IDIR Directory containing the netCDF include file `netcdf.inc`. This will be the local directory if you are using the version of this file included in the distribution.

The first two items in the list above control the treatment of `*.F` files by the Fortran preprocessor. Compilation has been tested on several systems, and the `Makefile` contains some example options (commented out) from each of these systems, along with information on the operating system and compiler used. Simply type `make q-gcm` to compile, once you have edited the `Makefile` to suit your system.

The model has been run using both f77 and f90/f95 compilers. The model can run in parallel; instructions using the standard OpenMP API are included in the code. You will need to set a suitable compiler flag to enable these directives.

9.3 Structure of the code

The Q-GCM model consists of a main program and 41 subprograms, 9 of which remain with the main program in the file `q-gcm.F`, 32 having been separated out into other `*.f` files. Below is a list showing where to find subroutines in the `*.f` files:

`q-gcm.F`	contains `qcomp`, `mqa`, `defrad`, `xintt`, `xintp`, `trapin`, `zeroin`, `rbalin`, `resave` (9)
`amlsubs.f`	contains `aml`, `amladv`, `amldif` (3)
`areasubs.F`	contains `areavg`, `areint` (2)
`atisubs.f`	contains `atinvq`, `chsolv` (2)
`diasubs.f`	contains `diagno`, `del4bx`, `del4ch`, `genint` (4)
`ocisubs.f`	contains `ocinvq`, `solb` (2)
`omlsubs.f`	contains `oml`, `omladv`, `omldif` (3)
`qgasubs.f`	contains `qgastep`, `atjacn`, `atfric` (3)
`qgosubs.f`	contains `qgostep`, `ocjacn`, `ocfric` (3)
`tavsubs.F`	contains `tavini`, `tavatm`, `tavocn`, `tavout` (4)
`xfosubs.F`	contains `xforc`, `function fsprim`, `bilint` (3)
	`atqzbd.f`, `ocqbdy.f` and `valids.f` are single routine files (3)

In addition there are Fourier transform library routines from FFTPACK, and some netCDF output routines, not counted above. All real variables are explicitly of Fortran type "double precision" (64 bit), giving a precision of 15 significant figures

9.3.1 Input files

Variables governing the model run are contained in two separate files, both of which are picked up by the main program file `q-gcm.f` via `INCLUDE` statements. These are the files to edit to change the model configuration from the default case.

parameter.src This contains dimensioning information for the model arrays, and defines the location of the oceanic domain within the atmospheric, and the relative resolutions of the two grids. It also contains the rotation parameters which define the latitude of the domains. The file also contains an explanation of all the parameters defined therein.

in_param.f A file defining the values of all other model parameters, both physical parameters, and control parameters for length of run, diagnostic intervals, etc. Also controls the directory to which output files are written. All definitions are in the form of Fortran assign statements. The file includes brief comments explaining the meaning of each parameter, including its units.

Both of these files are compiled as part of the program, so changes will only take effect after re-compilation. All these parameters (and many derived quantities) are written to standard output by the main program at the start of a run.

9.3.2 Program structure

A general idea of the structure of the code can be seen in the flow chart in figure 3. This shows the flow of control through the most important subroutines, and which equations they solve. Note that each `*.f` file may contain more than one subroutine (see the earlier list), but they are grouped logically, and well commented to describe their function.

9.3.3 Output files

Output files are stored in the directory specified in the variable `outdir` on the first line of `in_param.f`. The filenames are hardwired into the code, and therefore can only be

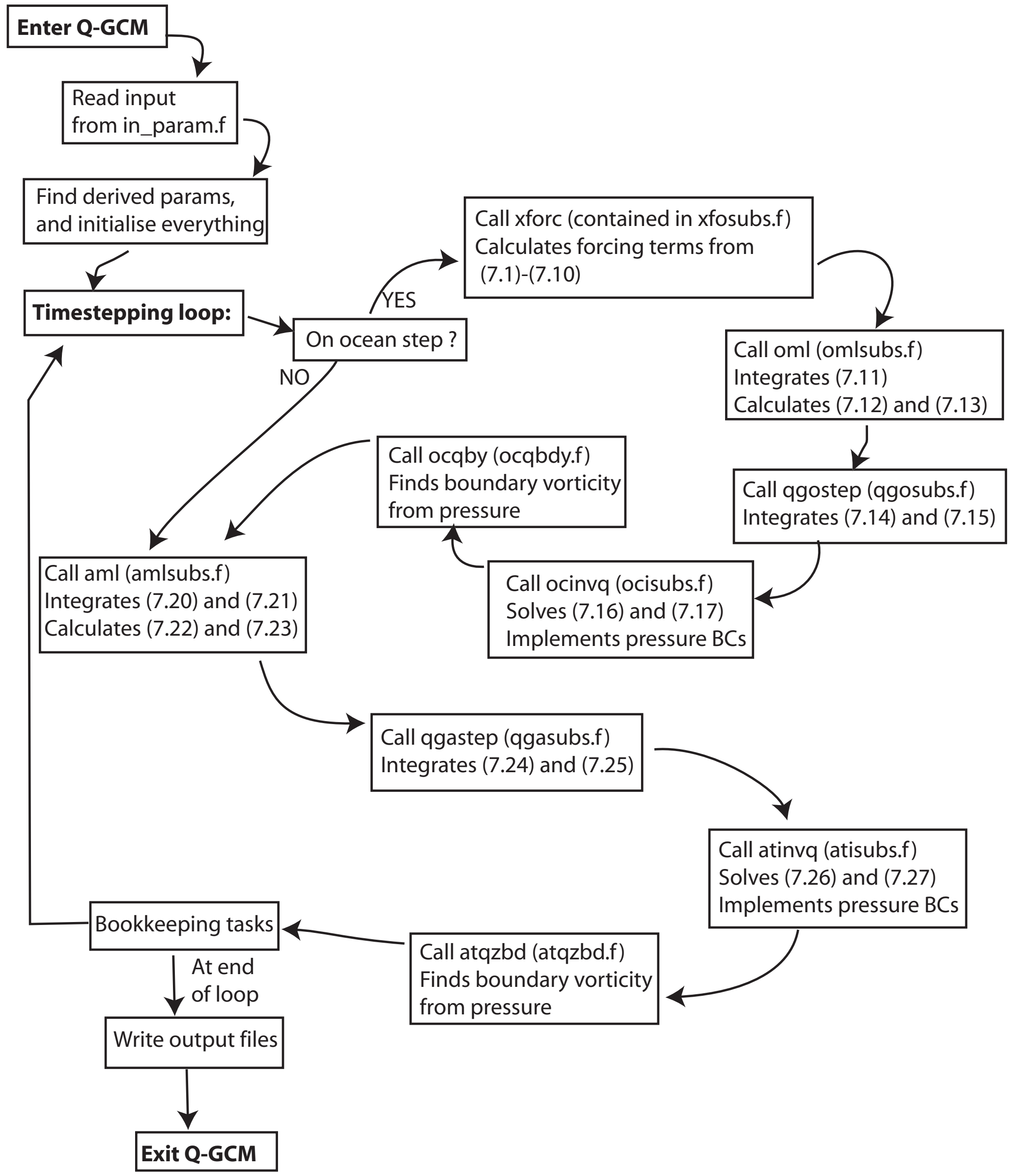

Figure 3: Flow chart showing the major subroutines of the code.

changed by altering the body of the code itself. Many of the file formats are in netCDF (`*.nc`) format, so that a description of variable names and units is included in the data file. The files are listed as follows:

input_parameters.m A file which includes all the parameters as a matlab script. Simply run this script in matlab, and variable names and values will be initialised.

restart A binary file written periodically which includes the model state variables. This can be useful for restarting the run if the model crashes part-way through.

last.day A binary file written at the end of the model run which can be used for continuing the run.

monit.nc A netCDF format file which includes timeseries of some important quantities.

atast.nc, atpa.nc Two netCDF data files which describe the atmospheric state. The variables written to these files is controlled by the `outflag` array in `in_param.f`.

ocsst.nc, ocpo.nc Two netCDF data files which describe the oceanic state. The variables written to these files is controlled by the `outflag` array in `in_param.f`.

avges.nc A netCDF data file which includes data averaged over the entire run.

9.3.4 Location of variables

Where possible variables are held in common blocks, rather than being passed as arguments to subroutines. Each common block is defined in a separate `*.cmn` file, which contains comments describing the meaning of each variable, and its units. Each of the 15 common blocks contains a set of related variables thus:

`atconst.cmn`	Time independent atmospheric parameters
`athomog.cmn`	Homogeneous atmospheric solutions and their coefficients
`atmfft.cmn`	Atmospheric Fourier transform coefficients
`atnc.cmn`	Identifiers for netCDF dumps of atmospheric variables
`atstate.cmn`	Time varying atmospheric state (pressure, vorticity, entrainment and Ekman velocity)
`intrfac.cmn`	All mixed layer parameters and variables, for both atmosphere and ocean, including dynamic stresses
`monitor.cmn`	Diagnostic quantities for monitoring model
`monnc.cmn`	Identifiers for netCDF dumps of diagnostic variables
`occonst.cmn`	Time independent oceanic parameters
`ochomog.cmn`	Homogeneous oceanic solution and its coefficients.
`ocnc.cmn`	Identifiers for netCDF dumps of oceanic variables
`ocnfft.cmn`	Oceanic Fourier sine transform coefficients
`ocstate.cmn`	Time varying oceanic state (pressure, vorticity, entrainment and Ekman velocity)
`radiate.cmn`	Radiation parameters needed by subroutines
`timavge.cmn`	Used for averaging fields over the course of a run

These files are included at the start of those subroutines where they are required. They are all included in the main program, to ensure that the values of their contents remain defined at all times. Variables declared within subroutines are purely local, so “stack” storage can be used to save memory.

9.3.5 Diagnostics

Where possible, instantaneous diagnostic quantities are computed by subroutine `diagno`, whose calling frequency is determined by the variable `dgnday`, set in `in_param.f`. One exception to this is that some quantities which would require inconvenient duplication of code are computed by the timestepping routines. Another exception is that convection-related quantities need to be computed in the timestepping subroutines, before convective adjustment is finally applied. These diagnostic quantities are all stored in the common block `monitor.cmn`, and output in netCDF format by subroutine `monnc_out`. Time averaged quantities are accumulated by subroutines `tavatm` and `tavocn` in the common block `timavge.cmn`, and finally computed and output by subroutine `tavout`.

9.3.6 Default case

The input files are supplied set to run a standard spin-up case with an ocean of 257×401 points and resolution 15 km, and an atmosphere of 128×67 points and resolution 120 km.

Each has 2 QG layers. This is the spin-up calculation described and illustrated in section 3 of Hogg et al. (2003). This case requires about 49 Mbyte of store for static storage, or about 26 Mbyte for stack storage.

9.3.7 Possible problems

- The program uses significant "stack" memory which may exceed the default on your system. You will need to reset this using the `limit stacksize` command.

9.3.8 Feedback and future plans

The model conforms strictly to Fortran standards, and so should be highly portable. It has been checked using the public domain Fortran77 analyzer "ftnchek", which we highly recommend. The home website is:
`http://dsm.dsm.fordham.edu/~ftnchek/`.
This software is also available from the Netlib software repository and its many mirror sites.

Please report any compilation or runtime problems, with details of the operating system and compiler used.

A Writing radiation as a perturbation to mean state

A.1 Functional form of radiation parameters

To determine radiation in the model we need prior knowledge of several functions. Firstly, the transmissivity τ is written as

$$\tau^{\uparrow}(z,h) = e^{-\frac{h-z}{z_0}}, \tag{A.1}$$

or

$$\tau^{\downarrow}(z,h) = e^{\frac{h-z}{z_0}}. \tag{A.2}$$

Derivatives of the transmissivities are then

$$\tau_z^{\uparrow}(z,h) = \frac{\tau^{\uparrow}(z,h)}{z_0}, \tag{A.3}$$

or

$$\tau_z^{\downarrow}(z,h) = \frac{-\tau^{\downarrow}(z,h)}{z_0}. \tag{A.4}$$

In the model, the optical depth z_0 will vary with height. We assume for now that we know the optical depth in the region of each interface (z_i).

Secondly, we need to know the radiation functions for each layer which are written

$$B_m(z) = \frac{\sigma}{2}(\overline{{}^aT_m} + {}^aT_m{}' - \gamma z)^4, \tag{A.5}$$

for the mixed layer, and

$$B_i(z) = \frac{\sigma}{2}({}^aT_i - \gamma z)^4, \tag{A.6}$$

for $i = 1, 2$. The terms in the temperature function represent constant potential temperature, the variation of in situ temperature with height (dependent upon the adiabatic lapse rate γ).

A.2 Rules for linearising

We want to linearise the radiation equations about a mean state. To do this we expand about a mean and retain the first order terms in ${}^aT_m{}'$, ${}^a\eta_m$ and ${}^a\eta_1$. For the mixed layer radiation function

$$\frac{\sigma}{2}(\overline{{}^aT_m} - \gamma z + {}^aT_m{}')^4 \approx \frac{\sigma}{2}(\overline{{}^aT_m} - \gamma z)^4 + 2\sigma(\overline{{}^aT_m} - \gamma z)^3\,{}^aT_m{}'. \tag{A.7}$$

Transmissivities are expanded by writing, for example,

$$\begin{aligned}
\tau^{\uparrow}({}^ah_m, {}^ah_1) &= e^{-\frac{{}^ah_1 - {}^ah_m}{z_1}} \\
&= e^{-\frac{{}^aH_1 + {}^a\eta_1 - {}^aH_m - {}^a\eta_m}{z_1}} \\
&= e^{-\frac{{}^aH_1 - {}^aH_m}{z_1}} e^{-\frac{{}^a\eta_1}{z_1}} e^{\frac{{}^a\eta_m}{z_1}} \\
&\approx \tau_1^{\uparrow}\left(1 - \frac{{}^a\eta_1}{z_1}\right)\left(1 + \frac{{}^a\eta_m}{z_1}\right) \\
&\approx \tau_1^{\uparrow}\left(1 - \frac{{}^a\eta_1}{z_1} + \frac{{}^a\eta_m}{z_1}\right)
\end{aligned} \tag{A.8}$$

where $\tau_1^{\uparrow} \equiv e^{-\frac{{}^aH_1 - {}^aH_m}{z_1}}$. Likewise

$$\tau^{\downarrow}({}^ah_1, {}^ah_m) \approx \tau_1^{\downarrow}\left(1 - \frac{{}^a\eta_1}{z_m} + \frac{{}^a\eta_m}{z_m}\right) \tag{A.9}$$

where $\tau_1^{\downarrow} \equiv e^{\frac{{}^aH_m - {}^aH_1}{z_m}}$. In addition we write integrations as

$$\int_{{}^ah_m}^{{}^ah_1} f(z)dz = \int_{{}^aH_m}^{{}^aH_1} f(z)dz - f({}^aH_m)^a\eta_m + f({}^aH_1)^a\eta_1. \tag{A.10}$$

A.3 Calculations

Atmospheric Mixed Layer

$$\begin{aligned}
F_m^{\uparrow} &= \int_0^{{}^ah_m} B_m(z)\tau_z^{\uparrow}(z, {}^ah_m)dz \\
&\approx \int_0^{{}^aH_m} B_m(z)\tau_z^{\uparrow}(z, {}^ah_m)\, dz + B_m({}^aH_m)\tau_z^{\uparrow}({}^aH_m, {}^ah_m)^a\eta_m \\
&\approx \int_0^{{}^aH_m} \left(\frac{\sigma}{2}(\overline{{}^aT_m} - \gamma z)^4 + 2\sigma\left(\overline{{}^aT_m} - \gamma z\right)^3 {}^aT_m{}'\right) \frac{e^{-\frac{{}^aH_m - z}{\bar{z_m}}}}{\bar{z_m}} \left(1 - \frac{{}^a\eta_m}{\bar{z_m}}\right) dz \\
&\quad + \frac{\sigma}{2}\left(\overline{{}^aT_m} - \gamma {}^aH_m\right)^4 \frac{1}{\bar{z_m}} {}^a\eta_m \\
&\approx \frac{\sigma}{2\bar{z_m}} \int_0^{{}^aH_m} \left(\overline{{}^aT_m} - \gamma z\right)^4 e^{-\frac{{}^aH_m - z}{\bar{z_m}}}\, dz \\
&\quad + \left(\frac{2\sigma}{\bar{z_m}} \int_0^{{}^aH_m} \left(\overline{{}^aT_m} - \gamma z\right)^3 e^{-\frac{{}^aH_m - z}{\bar{z_m}}}\, dz\right) {}^aT_m{}' \\
&\quad + \left(\frac{\sigma}{2\bar{z_m}}(\overline{{}^aT_m} - \gamma {}^aH_m)^4 - \frac{\sigma}{2\bar{z_m}^2} \int_0^{{}^aH_m} \left(\overline{{}^aT_m} - \gamma z\right)^4 e^{-\frac{{}^aH_m - z}{\bar{z_m}}}\, dz\right) {}^a\eta_m.
\end{aligned} \tag{A.11}$$

Downgoing radiation can be calculated simply using the assumption $z_0 = 0$, giving

$$\begin{aligned}
F_m^{\downarrow} &= \int_0^{{}^ah_m} B_m(z)\tau_z^{\downarrow}(z, 0)\, dz \\
&\approx \int_0^{{}^aH_m} B_m(z)\tau_z^{\downarrow}(z, 0)\, dz + B_m({}^aH_m)\tau_z^{\downarrow}({}^ah_m, 0)^a\eta_m \\
&\approx \int_0^{{}^aH_m} \left(\frac{\sigma}{2}\left(\overline{{}^aT_m} - \gamma z\right)^4 + 2\sigma\left(\overline{{}^aT_m} - \gamma z\right)^3 {}^aT_m{}'\right) \frac{-e^{-\frac{z}{z_0}}}{z_0}\, dz \\
&\quad + \frac{\sigma}{2}\left(\overline{{}^aT_m} - \gamma {}^aH_m\right)^4 \frac{-e^{-\frac{{}^aH_m}{z_0}}}{z_0} {}^a\eta_m \\
&\approx -\int_0^{{}^aH_m} \left(\frac{\sigma}{2}(\overline{{}^aT_m} - \gamma z)^4 + 2\sigma(\overline{{}^aT_m} - \gamma z)^{3a}T_m{}'\right)\delta(z)\, dz \\
&= -\frac{\sigma}{2}\overline{{}^aT_m}^4 - 2\sigma\overline{{}^aT_m}^{3a}T_m{}'
\end{aligned} \tag{A.12}$$

Lower Troposphere

$$\begin{aligned}
F_1^{\uparrow} &= F_m^{\uparrow}\tau^{\uparrow}({}^a h_m, {}^a h_1) + \int_{{}^a h_m}^{{}^a h_1} B_1(z)\tau_z^{\uparrow}(z, {}^a h_1)\, dz \\
&\approx \left(\overline{F_m^{\uparrow}} + B_m^{\uparrow}\, {}^a\eta_m + D_m^{\uparrow}\, {}^a T_m{}'\right)\tau_1^{\uparrow}\left(1 + \frac{{}^a\eta_m}{z_1} - \frac{{}^a\eta_1}{z_1}\right) \\
&\quad + \int_{{}^a H_m}^{{}^a H_1} \frac{\sigma}{2}({}^a T_1 - \gamma z)^4 \frac{e^{-\frac{{}^a H_1 - z}{z_1}}}{z_1}\left(1 - \frac{{}^a\eta_1}{z_1}\right) dz \\
&\quad - \frac{\sigma}{2}({}^a T_1 - \gamma\, {}^a H_m)^4 \frac{\tau_1^{\uparrow}}{z_1}\, {}^a\eta_m + \frac{\sigma}{2}({}^a T_1 - \gamma\, {}^a H_1)^4 \frac{1}{z_1}\, {}^a\eta_1 \\
&\approx \overline{F_m^{\uparrow}}\tau_1^{\uparrow} + \frac{\sigma}{2z_1}\int_{{}^a H_m}^{{}^a H_1} ({}^a T_1 - \gamma z)^4 e^{-\frac{{}^a H_1 - z}{z_1}}\, dz \\
&\quad + \tau_1^{\uparrow}\left(\frac{\overline{F_m^{\uparrow}}}{z_1} + B_m^{\uparrow} - \frac{\sigma}{2z_1}({}^a T_1 - \gamma\, {}^a H_m)^4\right){}^a\eta_m \\
&\quad + \left(-\frac{\overline{F_m^{\uparrow}}\tau_1^{\uparrow}}{z_1} + \frac{\sigma}{2z_1}({}^a T_1 - \gamma\, {}^a H_1)^4 - \frac{\sigma}{2z_1^2}\int_{{}^a H_m}^{{}^a H_1} ({}^a T_1 - \gamma z)^4 e^{-\frac{{}^a H_1 - z}{z_1}}\, dz\right){}^a\eta_1 \\
&\quad + \left(D_m^{\uparrow}\tau_1^{\uparrow}\right){}^a T_m{}'
\end{aligned} \tag{A.13}$$

For downgoing radiation,

$$\begin{aligned}
F_1^{\downarrow} &= F_2^{\downarrow}\tau^{\downarrow}({}^a h_1, {}^a h_m) + \int_{{}^a h_m}^{{}^a h_1} B_1(z)\tau_z^{\downarrow}(z, {}^a h_m)\, dz \\
&\approx \left(\overline{F_2^{\downarrow}} + A_2^{\downarrow}\, {}^a\eta_1\right)\tau_1^{\downarrow}\left(1 + \frac{{}^a\eta_m}{z_m^+} - \frac{{}^a\eta_1}{z_m^+}\right) \\
&\quad - \int_{{}^a H_m}^{{}^a H_1} \frac{\sigma}{2}({}^a T_1 - \gamma z)^4 \frac{e^{\frac{{}^a H_m - z}{z_m^+}}}{z_m^+}\left(1 + \frac{{}^a\eta_m}{z_m^+}\right) dz \\
&\quad + \frac{\sigma}{2}({}^a T_1 - \gamma\, {}^a H_m)^4 \frac{{}^a\eta_m}{z_m^+} - \frac{\sigma}{2}({}^a T_1 - \gamma\, {}^a H_1)^4 \frac{\tau_1^{\downarrow}}{z_m^+}\, {}^a\eta_1 \\
&\approx \left(\overline{F_2^{\downarrow}}\tau_1^{\downarrow} - \frac{\sigma}{2z_m^+}\int_{{}^a H_m}^{{}^a H_1} ({}^a T_1 - \gamma z)^4 e^{\frac{{}^a H_m - z}{z_m^+}}\, dz\right) \\
&\quad + \tau_1^{\downarrow}\left(-\frac{\overline{F_2^{\downarrow}}}{z_m^+} + A_2^{\downarrow} - \frac{\sigma}{2z_m^+}({}^a T_1 - \gamma\, {}^a H_1)^4\right){}^a\eta_1 \\
&\quad + \left(\frac{\overline{F_2^{\downarrow}}\tau_1^{\downarrow}}{z_m^+} + \frac{\sigma}{2z_m^+}({}^a T_1 - \gamma\, {}^a H_m)^4 - \frac{\sigma}{2{z_m^+}^2}\int_{{}^a H_m}^{{}^a H_1} ({}^a T_1 - \gamma z)^4 e^{\frac{{}^a H_m - z}{z_m^+}}\, dz\right){}^a\eta_m
\end{aligned} \tag{A.14}$$

Upper Troposphere

$$
\begin{aligned}
F_2^{\uparrow} &= F_1^{\uparrow}\tau^{\uparrow}({}^ah_1, {}^aH_T) + \int_{{}^ah_1}^{{}^aH_T} B_2(z)\tau_z^{\uparrow}(z, {}^aH_T)\,dz, \\
&\approx \left(\overline{F_1^{\uparrow}} + A_1^{\uparrow}{}^a\eta_1 + B_1^{\uparrow}{}^a\eta_m + D_1^{\uparrow}{}^aT_m{}'\right)\tau_2^{\uparrow}\left(1 + \frac{{}^a\eta_1}{z_2}\right) \\
&\quad + \int_{{}^aH_1}^{{}^aH_T} \frac{\sigma}{2}({}^aT_2 - \gamma z)^4 \frac{e^{-\frac{{}^aH_T - z}{z_2}}}{z_2}\,dz - \frac{\sigma}{2}({}^aT_2 - \gamma^a H_1)^4 \frac{\tau_2^{\uparrow}}{z_2}{}^a\eta_1 \\
&\approx \left(\overline{F_1^{\uparrow}}\tau_2^{\uparrow} + \frac{\sigma}{2z_2}\int_{{}^aH_1}^{{}^aH_T}({}^aT_2 - \gamma z)^4 e^{-\frac{{}^aH_T - z}{z_2}}\,dz\right) + B_1^{\uparrow}\tau_2^{\uparrow}{}^a\eta_m \\
&\quad + \tau_2^{\uparrow}\left(\frac{\overline{F_1^{\uparrow}}}{z_2} + A_1^{\uparrow} - \frac{\sigma}{2z_2}({}^aT_2 - \gamma^a H_1)^4\right){}^a\eta_1 + D_1^{\uparrow}\tau_2^{\uparrow}{}^aT_m{}'
\end{aligned}
\tag{A.15}
$$

For downgoing radiation,

$$
\begin{aligned}
F_2^{\downarrow} &= \int_{{}^ah_1}^{{}^aH_T} B_2(z)\tau_z^{\downarrow}(z, {}^ah_1)\,dz \\
&\approx -\int_{{}^aH_1}^{{}^aH_T} \frac{\sigma}{2}({}^aT_2 - \gamma z)^4 \frac{e^{\frac{{}^aH_1 - z}{z_1}}}{z_1}\left(1 + \frac{{}^a\eta_1}{z_1}\right)dz + \frac{\sigma}{2}({}^aT_2 - \gamma^a H_1)^4 \frac{{}^a\eta_1}{z_1} \\
&\approx -\frac{\sigma}{2z_1}\int_{{}^aH_1}^{{}^aH_T}({}^aT_2 - \gamma z)^4 e^{\frac{{}^aH_1 - z}{z_1}}\,dz \\
&\quad + \frac{\sigma}{2z_1}\left(-\frac{1}{z_1}\int_{{}^aH_1}^{{}^aH_T}({}^aT_2 - \gamma z)^4 e^{\frac{{}^aH_1 - z}{z_1}}\,dz + ({}^aT_2 - \gamma^a H_1)^4\right){}^a\eta_1
\end{aligned}
\tag{A.16}
$$

B Constraints on mass and momentum

B.1 Ocean constraints

The ocean is required to conserve mass, so that the area integrated change in layer height is purely driven by entrainment (as advective terms cancel). This gives the equation

$$\iint {}^o\eta_{1t}\,dA = -\iint {}^oe_1\,dA \tag{B.1}$$

which is the only constraint we apply. There is no momentum constraint to satisfy as the basin is closed.

B.2 Atmospheric momentum constraints

Following McWilliams (1977) we need 3 constraints on momentum. Two of these are constraints on the baroclinic mode, and one on the barotropic mode. To determine these constraints in the continuous case, we integrate (5.10) over the entire basin area A,

$$
\begin{aligned}
&\iint \nabla_H^2 {}^ap_{1t}\,dA - \frac{f_0^2}{{}^aH_1}\iint {}^a\eta_{1t}\,dA + f_0\iint\left(({}^au_1{}^aq_1)_x + ({}^av_1{}^aq_1)_y\right)dA \\
&\qquad = \frac{f_0^2}{{}^aH_1}\iint({}^ae_1 - {}^aw_{ek})\,dA - {}^aA_H\iint \nabla_H^6 {}^ap_1\,dA.
\end{aligned}
\tag{B.2}
$$

We apply a mass constraint

$$\iint {}^a\eta_{1t}\,dA = -\iint {}^ae_1\,dA, \tag{B.3}$$

and require that there is no net advection over the basin,

$$\iint \nabla_H^2 {}^a p_{1t}\, dA = -\frac{f_0^2}{{}^a H_1} \iint {}^a w_{ek}\, dA - {}^a A_H \iint \nabla_H^6 {}^a p_1\, dA. \tag{B.4}$$

This equation can be simplified by writing

$$\iint \nabla.(\nabla^a p_{1t})\, dA = -\frac{f_0}{{}^a H_1} \iint \nabla \times \tau\, dA - {}^a A_H \iint \nabla.\nabla(\nabla_H^4 {}^a p_1)\, dA \tag{B.5}$$

so that application of Gauss' and Stokes' theorem in a periodic channel gives

$$\int \left[{}^a p_{1yt}\right]_0^{L_y} dx = \frac{f_0}{{}^a H_1} \int \left[{}^a \tau^x\right]_0^{L_y} dx - {}^a A_H \int \left[\nabla_H^4 {}^a p_{1y}\right]_0^{L_y} dx, \tag{B.6}$$

where the square brackets refers to the difference between the values of the variables within at the north and south of the domain. The equivalent equation in layer 2 is simply

$$\int \left[{}^a p_{2yt}\right]_0^{L_y} dx = -{}^a A_H \int \left[\nabla_H^4 {}^a p_{2y}\right]_0^{L_y} dx. \tag{B.7}$$

The same equations can be written for the discrete case, however we only solve the vorticity evolution equation at internal points in the domain. Therefore we integrate only over the internal points (area A_I)

$$\begin{aligned}\iint \nabla_H^2 {}^a p_{1t}\, dA_I - \frac{f_0^2}{{}^a H_1} \iint {}^a \eta_{1t}\, dA_I + f_0 \iint \left(({}^a u_1 {}^a q_1)_x + ({}^a v_1 {}^a q_1)_y\right) dA_I \\ = \frac{f_0^2}{{}^a H_1} \iint ({}^a e_1 - {}^a w_{ek})\, dA_I - {}^a A_H \iint \nabla_H^6 {}^a p_1\, dA_I \end{aligned} \tag{B.8}$$

and note that there remain finite contributions from the advection terms and the mass balance. This contributions are simplified using

$$\begin{aligned}\iint ({}^a \eta_{1t} + {}^a e_1)\, dA = \iint ({}^a \eta_{1t} + {}^a e_1)\, dA_I \\ + \frac{\Delta y}{2} \int \left[({}^a \eta_{1t} + {}^a e_1)^{(1)} + ({}^a \eta_{1t} + {}^a e_1)^{(n)}\right] dx = 0, \end{aligned} \tag{B.9}$$

giving

$$\iint ({}^a \eta_{1t} + {}^a e_1)\, dA_I = -\frac{\Delta y}{2} \int \left[({}^a \eta_{1t} + {}^a e_1)^{(1)} + ({}^a \eta_{1t} + {}^a e_1)^{(n)}\right] dx. \tag{B.10}$$

Here the bracketed superscripts refer to the value of the quantity at that gridpoint. We can do the same thing for the advective contributions,

$$\iint \left(({}^a u_1 {}^a q_1)_x + ({}^a v_1 {}^a q_1)_y\right) dA_I = -\int \left(J_1^{(1)} + J_1^{(n)}\right) dx. \tag{B.11}$$

where J_i is the evaluation of the Jacobian advection scheme at the boundary point of layer i.

Following McWilliams (1977) we choose to satisfy constraints along each of the north and south boundaries indpendently. We gather all the terms in (B.8) and write two equations,

$$\begin{aligned}\int {}^a p_{1yt}^{(1.5)}\, dx - \frac{f_0^2 \Delta y}{2 {}^a H_1} \int {}^a \eta_{1t}^{(1)}\, dx \\ = -f_0 \int J_1^{(1)}\, dx + \frac{f_0^2 \Delta y}{2 {}^a H_1} \int {}^a e_1^{(1)}\, dx + \frac{f_0}{{}^a H_1} \int {}^a \tau^{x(1.5)}\, dx - {}^a A_H \int {}^a p_{15y}^{(1.5)}\, dx, \end{aligned} \tag{B.12}$$

$$\int {}^a p_{1\,yt}^{(n-0.5)}\,dx + \frac{f_0^2\Delta y}{2\,{}^aH_1}\int {}^a\eta_{1\,t}^{(n)}\,dx = f_0\int J_1^{(n)}\,dx - \frac{f_0^2\Delta y}{2\,{}^aH_1}\int {}^ae_1{}^{(n)}\,dx + \frac{f_0}{{}^aH_1}\int {}^a\tau^{x(n-0.5)}\,dx - {}^aA_H\int {}^ap_{1\,5y}^{(n-0.5)}\,dx. \quad \text{(B.13)}$$

The equivalent equations for the upper layer are

$$\int {}^a p_{2\,yt}^{(1.5)}\,dx + \frac{f_0^2\Delta y}{2\,{}^aH_2}\int {}^a\eta_{1\,t}^{(1)}\,dx = -f_0\int J_2^{(1)}\,dx - \frac{f_0^2\Delta y}{2\,{}^aH_2}\int {}^ae_1{}^{(1)}\,dx - {}^aA_H\int {}^ap_{2\,5y}^{(1.5)}\,dx, \quad \text{(B.14)}$$

$$\int {}^a p_{2\,yt}^{(n-0.5)}\,dx - \frac{f_0^2\Delta y}{2\,{}^aH_2}\int {}^a\eta_{1\,t}^{(n)}\,dx = f_0\int J_2^{(n)}\,dx + \frac{f_0^2\Delta y}{2\,{}^aH_2}\int {}^ae_1{}^{(n)}\,dx - {}^aA_H\int {}^ap_{2\,5y}^{(n-0.5)}\,dx. \quad \text{(B.15)}$$

Equations (B.12)–(B.15) can now be combined to give Southern and Northern baroclinic constraints (${}^ap_c{}^{1(P)}$ and ${}^ap_c{}^{n(P)}$), and a Southern barotropic constraint (${}^ap_b{}^{1(P)}$). Firstly take $(B.12) - (B.14)$:

$$\left(\int {}^ap_{c\,y}^{(1.5)}\,dx - \frac{f_0^2\Delta y}{2\,{}^ag'}\left(\frac{1}{{}^aH_1}+\frac{1}{{}^aH_2}\right)\int {}^ap_c{}^{(1)}\,dx\right)_t = f_0\int\left(J_2^{(1)} - J_1^{(1)}\right)dx + \frac{f_0^2\Delta y}{2}\left(\frac{1}{{}^aH_1}+\frac{1}{{}^aH_2}\right)\int {}^ae_1{}^{(1)}\,dx + \frac{f_0}{{}^aH_1}\int {}^a\tau^{x(1.5)}\,dx - {}^aA_H\int {}^ap_{c\,5y}^{(1.5)}\,dx, \quad \text{(B.16)}$$

For the Northern condition, $(B.13) - (B.15)$:

$$\left(\int {}^ap_{c\,y}^{(n-0.5)}\,dx + \frac{f_0^2\Delta y}{2\,{}^ag'}\left(\frac{1}{{}^aH_1}+\frac{1}{{}^aH_2}\right)\int {}^a\eta_1{}^{(n)}\,dx\right)_t = f_0\int (J_1^{(n)} - J_2^{(n)})\,dx - \frac{f_0^2\Delta y}{2}\left(\frac{1}{{}^aH_1}+\frac{1}{{}^aH_2}\right)\int {}^ae_1{}^{(n)}\,dx + \frac{f_0}{{}^aH_1}\int {}^a\tau^{x(n-0.5)}\,dx - {}^aA_H\int {}^ap_{c\,5y}^{(n-0.5)}\,dx. \quad \text{(B.17)}$$

For the barotropic condition, ${}^aH_1(B.12) + {}^aH_2(B.14)$:

$$\left(\int {}^ap_{b\,y}^{(1.5)}\,dx\right)_t = -f_0\int\left({}^aH_1J_1^{(1)} + {}^aH_2J_2^{(1)}\right)dx + f_0\int {}^a\tau^{x(1.5)}\,dx - {}^aA_H\int {}^ap_{b\,5y}^{(1.5)}\,dx. \quad \text{(B.18)}$$

C Application of boundary conditions

The boundary conditions in the model are described by (2.23)–(2.25). To apply these conditions at (say) the Southern boundary of the domain write the first order centred difference of pressure at the boundary to be

$$p_y^{(1)} = \frac{p^{(2)} - p^{(0)}}{2\Delta} \quad \text{(C.1)}$$

$$p_{yy}^{(1)} = \frac{p^{(2)} - 2p^{(1)} + p^{(0)}}{\Delta^2} \quad \text{(C.2)}$$

where $p^{(0)}$ is defined a be a point on the other side of the boundary and Δ the grid spacing. Using (2.24)

$$\frac{p^{(2)} - 2p^{(1)} + p^{(0)}}{\Delta^2} = \alpha \frac{p^{(2)} - p^{(0)}}{2\Delta} \tag{C.3}$$

which can be rewritten

$$p^{(0)} = \frac{(\frac{\alpha\Delta}{2} - 1)p^{(2)} + 2p^{(1)}}{\frac{\alpha\Delta}{2} + 1}. \tag{C.4}$$

The boundary derivatives can be restated as

$$p_y^{(1)} = \frac{p^{(2)} - p^{(1)}}{\Delta(\frac{\alpha\Delta}{2} + 1)} \tag{C.5}$$

$$p_{yy}^{(1)} = \frac{\alpha\Delta(p^{(2)} - p^{(1)})}{\Delta^2(\frac{\alpha\Delta}{2} + 1)}. \tag{C.6}$$

Likewise at the Northern boundary we can write

$$p_y^{(n)} = \frac{p^{(n)} - p^{(n-1)}}{\Delta(\frac{\alpha\Delta}{2} + 1)} \tag{C.7}$$

$$p_{yy}^{(n)} = \frac{\alpha\Delta(p^{(n-1)} - p^{(n)})}{\Delta^2(\frac{\alpha\Delta}{2} + 1)}. \tag{C.8}$$

At the Western boundary in the ocean, the condition is identical to the Southern condition (with y derivatives replaced by x), and Eastern boundaries are equivalent to Northern boundaries.

D Starting at radiative equilibrium

We can start at radiative equilibrium by writing

$${}^aF_m^T = 0 \tag{D.1}$$

$${}^oF_m^T = 0 \tag{D.2}$$

$${}^ae_1 = 0 \tag{D.3}$$

These can be used to find starting conditions for ${}^aT_m{}'$, ${}^oT_m{}'$ and ${}^a\eta_1$, and we assume ${}^o\eta_1 = 0$ and ${}^a\eta_m = 0$. We therefore set

$$0 = -A_1^{\downarrow}{}^a\eta_1 - D_m^{\uparrow}{}^aT_m{}' - F_s', \tag{D.4}$$

$$0 = (\lambda - D_m^{\downarrow}){}^aT_m{}' + (-\lambda - D_0^{\uparrow}){}^oT_m{}' - F_s', \tag{D.5}$$

$$0 = (A_1^{\downarrow} - A_2^{\uparrow}){}^a\eta_1 + (D_m^{\uparrow} - D_2^{\uparrow}){}^aT_m{}', \tag{D.6}$$

Using (D.4) and (D.6) we get

$${}^aT_m{}' = \frac{(A_1^{\downarrow} - A_2^{\uparrow})F_s'}{A_2^{\uparrow}D_m^{\uparrow} - A_1^{\downarrow}D_2^{\uparrow}}, \tag{D.7}$$

and feed this back into (D.6):

$${}^a\eta_1 = \frac{-(D_m^{\uparrow} - D_2^{\uparrow})F_s'}{A_2^{\uparrow}D_m^{\uparrow} - A_1^{\downarrow}D_2^{\uparrow}} \tag{D.8}$$

We then find ocean mixed layer temperature from (D.5):

$${}^oT_m{}' = \left(\frac{(\lambda - D_m^{\downarrow})(A_1^{\downarrow} - A_2^{\uparrow})}{A_2^{\uparrow}D_m^{\uparrow} - A_1^{\downarrow}D_2^{\uparrow}} - 1 \right) \frac{F_s'}{\lambda + D_0^{\uparrow}} \tag{D.9}$$

E Kinetic Energy

We start by considering the kinetic energy in atmosphere layer 1, which comes from equations (5.10)–(5.12). To find the total kinetic energy we multiply each layer by ${}^a p_1$ and integrate over the entire domain. Taking (5.10) we start with

$$\iint {}^a p_1 \left(\nabla_H^2 {}^a p_{1t} - \frac{f_0^2}{{}^a H_1} {}^a \eta_{1t}\right) dA = \frac{f_0^2}{{}^a H_1} \iint {}^a p_1 ({}^a e_1 - {}^a w_{ek})\, dA - {}^a A_H \iint {}^a p_1 \nabla_H^6 {}^a p_1 \, dA. \tag{E.1}$$

We want to make use of the constraints in Appendix B.2, and so we integrate these terms by parts where possible,

$$\iint {}^a p_1 ({}^a p_{1xxt} + {}^a p_{1yyt})\, dx\, dy = \frac{f_0^2}{{}^a H_1} \iint {}^a p_1 ({}^a \eta_{1t} + {}^a e_1)\, dx\, dy$$
$$- \frac{f_0}{{}^a H_1} \iint {}^a p_1 ({}^a \tau_x^y - {}^a \tau_y^x)\, dx\, dy - {}^a A_H \iint {}^a p_1 \nabla_H^4 ({}^a p_{1xx} + {}^a p_{1yy})\, dx\, dy. \tag{E.2}$$

$$\int \left([{}^a p_1 {}^a p_{1xt}]_0^{L_x} - \int {}^a p_{1x} {}^a p_{1xt}\, dx \right) dy + \int \left([{}^a p_1 {}^a p_{1yt}]_0^{L_y} - \int {}^a p_{1y} {}^a p_{1yt}\, dy \right) dx$$
$$= \frac{f_0^2}{{}^a H_1} \iint {}^a p_1 ({}^a \eta_{1t} + {}^a e_1)\, dx\, dy - \frac{f_0}{{}^a H_1} \int \left([{}^a p_1 {}^a \tau^y]_0^{L_x} - \int {}^a p_{1x} {}^a \tau^y \, dx \right) dy$$
$$+ \frac{f_0}{{}^a H_1} \int \left([{}^a p_1 {}^a \tau^x]_0^{L_y} - \int {}^a p_{1y} {}^a \tau^x \, dy \right) dx$$
$$- {}^a A_H \int \left([{}^a p_1 \nabla_H^4 {}^a p_{1x}]_0^{L_x} - \int {}^a p_{1x} \nabla_H^4 {}^a p_{1x}\, dx \right) dy$$
$$- {}^a A_H \int \left([{}^a p_1 \nabla_H^4 {}^a p_{1y}]_0^{L_y} - \int {}^a p_{1y} \nabla_H^4 {}^a p_{1y}\, dy \right) dx. \tag{E.3}$$

We simplify this expression by writing pressure gradients as geostrophic velocities to give

$$- \iint ({}^a v_1 {}^a v_{1t} + {}^a u_1 {}^a u_{1t})\, dA = \frac{1}{{}^a H_1} \iint {}^a p_1 ({}^a \eta_{1t} + {}^a e_1)\, dA$$
$$+ \frac{1}{{}^a H_1} \iint ({}^a v_1 {}^a \tau^y + {}^a u_1 {}^a \tau^x)\, dA + {}^a A_H \iint ({}^a v_1 \nabla_H^4 {}^a v_1 + {}^a u_1 \nabla_H^4 {}^a u_1)\, dA$$
$$- \frac{1}{f_0} \int \left[{}^a p_1 \left({}^a v_{1t} + \frac{{}^a \tau^y}{{}^a H_1} + {}^a A_H \nabla_H^4 {}^a v_1 \right) \right]_0^{L_x} dy$$
$$+ \frac{1}{f_0} \int \left[{}^a p_1 \left({}^a u_{1t} + \frac{{}^a \tau^x}{{}^a H_1} + {}^a A_H \nabla_H^4 {}^a u_1 \right) \right]_0^{L_y} dx. \tag{E.4}$$

We note again that jumps across a periodic domain must be zero so that the second last integral here disappears. In addition, the last integral can be cancelled using (B.6). We then define the kinetic energy ${}^a \mathrm{KE}_1 \equiv 0.5 {}^a \rho {}^a H_1 \iint ({}^a u_1{}^2 + {}^a v_1{}^2)\, dA$ (with units of energy per unit area), and the dissipation ${}^a \epsilon_1 \equiv {}^a A_H {}^a \rho {}^a H_1 \iint ({}^a v_1 \nabla_H^4 {}^a v_1 + {}^a u_1 \nabla_H^4 {}^a u_1)\, dA$ (with units of power per unit area) to write

$${}^a \mathrm{KE}_{1t} = -{}^a \rho \iint {}^a p_1 ({}^a \eta_{1t} + {}^a e_1)\, dA - {}^a \rho \iint ({}^a v_1 {}^a \tau^y + {}^a u_1 {}^a \tau^x)\, dA - {}^a \epsilon_1. \tag{E.5}$$

Here the first term on the right represents the production of kinetic energy by diabatic processes, and the second term represents the drag on the bottom of the atmosphere. The analogous equation for layer 2 in the atmosphere can be written

$${}^a \mathrm{KE}_{2t} = {}^a \rho \iint {}^a p_2 ({}^a \eta_{1t} + {}^a e_1)\, dA - {}^a \epsilon_2. \tag{E.6}$$

We repeat this exercise for the ocean, beginning with layer 1. Multiply (5.1) by ${}^o p_1$ and integrate over the ocean domain,

$$\iint {}^o p_1 \left(\nabla_H^2 {}^o p_{1t} + \frac{f_0^2}{{}^o H_1} {}^o \eta_{1t} \right) dA = \frac{f_0^2}{{}^o H_1} \iint {}^o p_1 ({}^o w_{ek} - {}^o e_1)\, dA - {}^o A_H \iint {}^o p_1 \nabla_H^6 {}^o p_1 \, dA. \tag{E.7}$$

The same manipulations can be used to write

$$\begin{aligned} {}^o\mathrm{KE}_{1t} = {}^o\rho \iint {}^o p_1 ({}^o\eta_{1t} + {}^o e_1)\, dA + {}^o\rho \iint \left({}^o v_1 {}^o\tau^y + {}^o u_1 {}^o \tau^x \right) dA - {}^a\epsilon_1 \\ - \frac{1}{f_0} \int \left[{}^o p_1 \left({}^o v_{1t} - \frac{{}^o\tau^y}{{}^o H_1} + {}^o A_H \nabla_H^4 {}^o v_1 \right) \right]_0^{L_x} dy \\ + \frac{1}{f_0} \int \left[{}^o p_1 \left({}^o u_{1t} - \frac{{}^o\tau^x}{{}^o H_1} + {}^o A_H \nabla_H^4 {}^o u_1 \right) \right]_0^{L_y} dx. \end{aligned} \tag{E.8}$$

In the ocean we cannot use periodic boundary conditions to elimate these integrals, and so integrate the vorticity equation to write

$$\begin{aligned} \iint \left({}^o p_{1xxt} + {}^o p_{1yyt} \right) dx\, dy \\ = \frac{f_0}{{}^o H_1} \iint \left({}^o\tau_x^y - {}^o\tau_y^x \right) dx\, dy - {}^o A_H \iint \nabla_H^4 ({}^o p_{1xx} + {}^o p_{1yy})\, dx\, dy. \end{aligned} \tag{E.9}$$

$$\int \left[{}^o v_{1t} - \frac{{}^o\tau^y}{{}^o H_1} + {}^o A_H \nabla_H^4 {}^o v_1 \right]_0^{L_x} dy - \int \left[{}^o u_{1t} - \frac{{}^o\tau^x}{{}^o H_1} + {}^o A_H \nabla_H^4 {}^o u_1 \right]_0^{L_y} dx = 0. \tag{E.10}$$

Since ${}^o p_1$ is constant on the boundaries, we have following ocean layer 1 kinetic energy equation,

$${}^o\mathrm{KE}_{1t} = {}^o\rho \iint {}^o p_1 ({}^o\eta_{1t} + {}^o e_1)\, dA + {}^o\rho \iint \left({}^o v_1 {}^o\tau^y + {}^o u_1 {}^o\tau^x \right) dA - {}^o\epsilon_1. \tag{E.11}$$

The layer 2 kinetic energy equation comes from

$$\begin{aligned} \iint {}^o p_2 \left(\nabla_H^2 {}^o p_{2t} - \frac{f_0^2}{{}^o H_2} {}^o\eta_{1t} \right) dA \\ = \frac{f_0^2}{{}^o H_2} \iint {}^o p_2 \left({}^o e_1 - \frac{\delta_e}{2 f_0} \nabla_h^2 {}^o p_2 \right) dA - {}^o A_H \iint {}^o p_2 \nabla_H^6 {}^o p_2 \, dA, \end{aligned} \tag{E.12}$$

and gives the equation

$${}^o\mathrm{KE}_{2t} = -{}^o\rho \iint {}^o p_2 ({}^o\eta_{1t} + {}^o e_1)\, dA - \frac{{}^o\rho \delta_e f_0}{2} \iint \left({}^o u_2{}^2 + {}^o v_2{}^2 \right) dA - {}^o\epsilon_2. \tag{E.13}$$

References

Arakawa, A. and Lamb, V. R. (1977). Computational design of the basic dynamical processes processes of the UCLA general circulation model. *Meth. Comp. Phys.*, 17:173–365.

Arakawa, A. and Lamb, V. R. (1981). A potential enstrophy and energy conserving scheme for the shallow water equations. *Mon. Weather Rev.*, 109:18–36.

Haidvogel, D. B., McWilliams, J. C., and Gent, P. R. (1992). Boundary current separation in a quasigeostrophic, eddy-resolving ocean circulation model. *J. Phys. Oceanogr.*, 22:882–902.

Hogg, A. M., Dewar, W. K., Killworth, P. D., and Blundell, J. R. (2003). A quasi-geostrophic coupled model: Q-GCM. *Mon. Weather Rev.* In Press. Available from http://www.soc.soton.ac.uk/JRD/PROC/Q-GCM/hoggetal2003.pdf.

Kravtsov, S. and Robertson, A. W. (2002). Midlatitude ocean-atmosphere interaction in an idealized coupled model. *Climate Dyn.*, 19:693–711.

McDougall, T. and Dewar, W. (1998). Vertical mixing and cabbeling in layered models. *J. Phys Oceanogr.*, 28:1458–1480.

McWilliams, J. C. (1977). A note on a consistent quasigeostrophic model in a multiply connected domain. *Dyn. Atmos. Oceans*, 1:427–441.

Opsteegh, J. D., Haarsma, R. J., Selten, F. M., and Kattenberg, A. (1998). ECBilt: a dynamic alternative to mixed boundary conditions in ocean models. *Tellus*, 50A:348–367.

Pedlosky, J. (1987). *Geophysical Fluid Dynamics*. Springer-Verlag.

Press, W. H., Teukolsky, S. A., Vetterling, W. T., and Flannery, B. P. (1992). *Numerical Recipes in Fortran 77: The Art of Scientific Computing (2nd ed.)*. Cambridge University Press.